Biosensors and Bioelectronics 178 (2021) 113030

Contents lists available at ScienceDirect

Biosensors and Bioelectronics

journal homepage: http://www.elsevier.com/locate/bios

G-quadruplex: Flexible conformational changes by cations, pH, crowding and its applications to biosensing

Maui Nishio, Kaori Tsukakoshi, Kazunori Ikebukuro *

Department of Biotechnology and Life Science, Tokyo University of Agriculture and Technology, 2-24-16 Naka-cho, Koganei, Tokyo, 184-8588, Japan

ARTICLE INFO

Keywords:
G-quadruplex
G4 topology
Aptamers
Biosensor

ABSTRACT

G-quadruplex (G4) is a non-canonical structure that is formed in G-rich sequences of nucleic acids. G4s play important roles *in vivo*, such as telomere maintenance, transcription, and DNA replication. There are three typical topologies of G4: parallel, anti-parallel, and hybrid. In general, metal cations, such as potassium and sodium, stabilize G4s through coordination in the G-quartet.

While G4s have some functions *in vivo*, there are many reports of developed applications that use G4s. As various conformations of G4s could form from one sequence depending on varying conditions, many researchers have developed G4-based sensors. Furthermore, G4 is a great scaffold of aptamers since many aptamers folded into G4s have also been reported. However, there are some challenges about its practical use due to the difference between practical sample conditions and experimental ones. G4 conformations are dramatically altered by the surrounding conditions, such as metal cations, pH, and crowding. Many studies have been conducted to characterize G4 conformations under various conditions, not only to use G4s in practical applications but also to reveal its function *in vivo*.

In this review, we summarize recent studies that have investigated the effects of surrounding conditions (e.g., metal cations, pH, and crowding) on G4 conformations and the application of G4s mainly in biosensor fields, and in others.

1. Introduction

Nucleic acids form various three-dimensional structures (Day et al., 2014; Frank-Kamenetskii et al., 2003; Frank-Kamenetskii and Mirkin, 1995). Single-stranded DNA or RNA can fold into canonical structures using the Watson-Crick base pairs and non-canonical structures (e.g., G-quadruplex and i-motif). These structures work in gene regulation and riboswitches *in vivo* and are applied in various devices such as aptamers and artificial riboswitches.

G-quadruplex (G4) is one kind of a non-canonical structure formed in G-rich sequences (Frank-Kamenetskii et al., 2003; Sen and Gilbert, 1988). G4 consists of more than two G-quartets, which are the planes formed by four bases of Gs via the Hoogsteen base pairs. G4s have topologies that are classified by the orientation of their loops such as parallel, anti-parallel, and hybrid. In general, G4s are stable in the presence of metal cations such as K^+ and Na^+ because these cations coordinate in the G-quartet (Phan, 2010). There are many reports that G4 forms *in vivo* as the telomeric sequence and oncogene promoters. These G4s have been suggested to play important roles *in vivo*, including replication, gene expression, telomere maintenance, and transcription (Maizels and Gray, 2013; Spiegel et al., 2020). For instance, G4s in telomeres inhibit the telomerase because of their three-dimensional structure (Zahler et al., 1991) but might work on telomerase recruitment (Moye et al., 2015). Some G4s in oncogene promoters were reported to regulate their gene expression (Brooks and Hurley, 2009; Cogoi and Xodo, 2006). The irregular formation of G4s on some genes might cause neurodegenerative diseases and cancers. Therefore, G4s in the genome are the therapeutic targets of these diseases.

Many G4 ligands have been developed to apply as drugs (Spiegel et al., 2020). For instance, cancer cells with lack of repair pathways are sensitive to G4 ligands such as pyridostatin (Rodriguez et al., 2012) and RHPS4 (Salvati et al., 2010). One of the G4 ligand MM41 was reported to cause 80% decrease in growth of tumor in *in vivo* model for pancreatic cancer (Ohnmacht et al., 2015). These studies suggest that G4-specific ligands could be applied to cancer therapy, especially in cancer cells, genetically lacking DNA damage repair (McLuckie et al., 2013; Zimmer et al., 2016). To further develop therapeutics, the functions of G4 *in vivo* should be elucidated in detail. Furthermore, it was reported that there

* Corresponding author.
E-mail address: ikebu@cc.tuat.ac.jp (K. Ikebukuro).

https://doi.org/10.1016/j.bios.2021.113030
Received 12 November 2020; Received in revised form 7 January 2021; Accepted 20 January 2021
Available online 23 January 2021

are 716,310 distinct G4 structures in the human genome, including oncogenes and tumor suppressors, identified by high-throughput sequencing (Chambers et al., 2015). This means that G4s might have a greater variety of roles *in vivo* than previously reported.

While the functions of G4s have been studied, many applications using G4s on biosensors and molecular devices have also been reported (Alberti and Mergny, 2003). Since various conformations of G4 could form from one sequence under different cationic conditions, many researchers have developed G4-based metal cation sensors (Zhou et al., 2017). There have also been reports of many G4-forming aptamers such as thrombin (Bock et al., 1992; Macaya et al., 1993), VEGF (Nonaka et al., 2010), Cry j 2 (Ogihara et al., 2015), insulin (Yoshida et al., 2009), *Fok*I (Nishio et al., 2017). Therefore, it is suggested that G4 is an excellent scaffold for aptamers. Since these G4-forming aptamers have high affinity and specificity, they can be used in various applications such as biosensors and protein delivery systems. G4s are used in these applications as recognition elements such as aptamers and signal generating elements (Fig. 1). There are mainly two types of signal generating element using G4 as labels: the peroxidase-like activity of the G4/hemin complex (Travascio et al., 1998) and the fluorescence by binding to G4-specific ligands (Mohanty et al., 2013; Umar et al., 2019). Meanwhile, there is an RNA aptamer with a G4 conformation that generates fluorescence like GFP when it binds to its target ligand, termed Spinach (Huang et al., 2014; Paige et al., 2011). It was also used in some applications (Burch et al., 2017; Dasgupta et al., 2015).

G4 conformations change dramatically based on the surrounding environment, such as cations, pH, crowding, and temperature. Therefore, despite having one kind of sequence, different G4 topologies or conformations can be observed (Nakano et al., 2014). Many studies have been performed on G4 conformation under various conditions using analytical methods such as nuclear magnetic resonance (NMR) (Adrian et al., 2012; Wang and Patel, 1992), circular dichroism (CD) spectroscopy (Chen, 1992; Paramasivan et al., 2007), mass spectroscopy (David et al., 2002; Li, 2019; Ma et al., 2019). However, some systems do not work well *in vivo* or with real samples because the surrounding conditions affect the conformation of G4 and it is difficult to control (Li et al, 2010, 2011, 2012). To unravel the functions of G4 *in vivo* and create effective designs of G4-forming sequences for applications, we need to completely understand how the environmental factors affect G4 conformations. Many studies have investigated G4 conformational changes in relation to temperature, to mainly study the stability of G4 conformations (Lane et al., 2008). Since temperature is an exceptional factor frequently used to investigate the stability of G4s, we focused on the chemical factors that affect G4 conformations in this review.

There are some reviews about G4-based biosensors (Roxo et al., 2019; Xi et al., 2020; Yang et al., 2020). They reviewed published G4-based biosensors and discuss their potential. Although G4 could change its conformation dramatically by environmental factors included the measurement samples, there are no reviews which overview the effects of these factors on G4. In this review, we have summarized from recent reports, the environmental factors, metal cations, crowding conditions, and pH that affect G4 conformation and how they change their conformation. We have also introduced recent applications using G4 mainly focused on the biosensor field, and on other applications and ways to improve G4 sequences for these applications. Finally, we would like to state the possibility of the applications using these conformational changes and discuss developing biosensors using G4s.

2. Conformational changes by surrounding conditions

In this section, we will first mention the fundamental topologies of G4 in section 2-1, and then review the conformational changes in G4 by surrounding conditions in section 2-2 to 2-5. We will focus on the three chemical factors that affect G4 conformations, metal cations, pH, and molecular crowding, and the other chemical factor, spermine.

2.1. Fundamental topologies of G4

Before reviewing the conformational changes in G4, we have reviewed the three kinds of G4 topologies (Ou et al., 2008). G4 can be intramolecular and intermolecular such as bimolecular and tetramolecular and there are mainly three types of topologies in G4: parallel, anti-parallel, and hybrid, classified by the orientation of their loops and G-tracts (Fig. 2a). The G-tract means continuous runs of guanine bases. In the parallel topologies, all chains consisting of G4 are parallel. Two chains are parallel in the anti-parallel topologies and one chain in the hybrid topologies. There are also some types of loops in G4 depending on the connection between the G-tracts, such as diagonal, lateral, and propeller (Fig. 2b). The chain connecting the G-main chain on the diagonal of the G-quartet is called as the diagonal loop. The lateral and propeller loops connect adjacent anti-parallel G-backbones and parallel G-main chains, respectively. In other words, the parallel G4s have three propeller loops, and the hybrid and anti-parallel G4s have both the lateral and the diagonal loops. The methods of analysis of G4 topologies

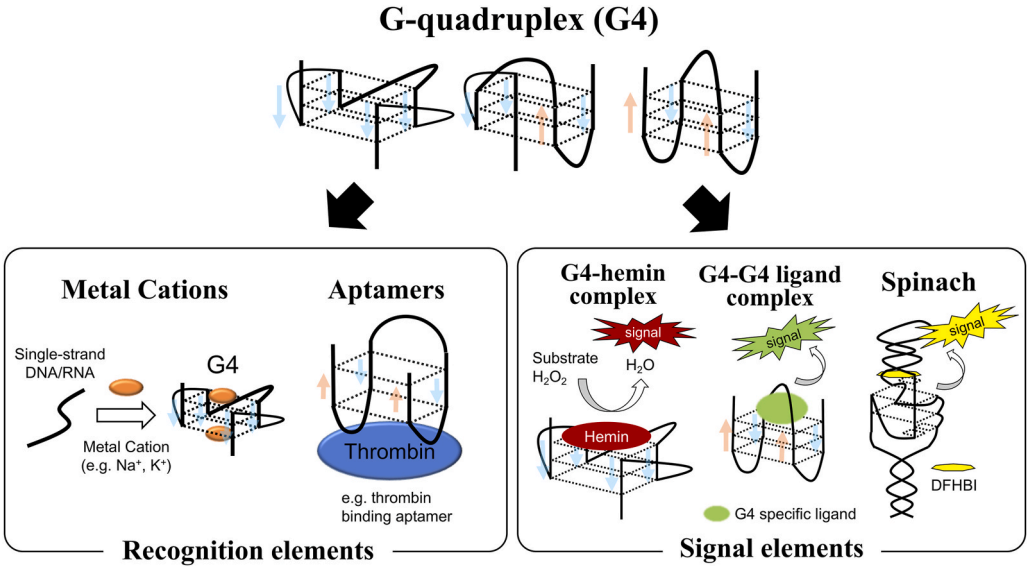

Fig. 1. Illustrations of G4 applications.

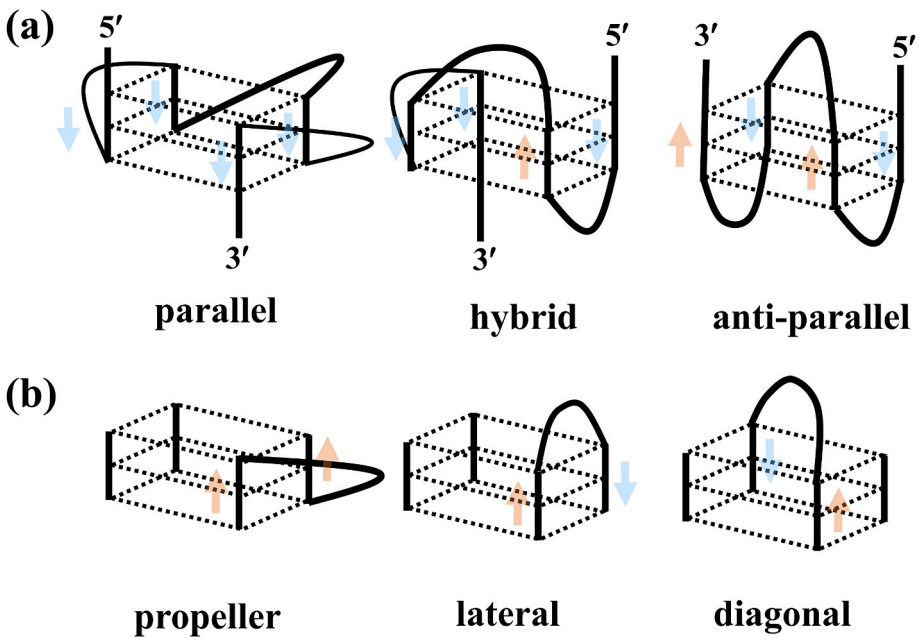

Fig. 2. Topologies of G4 (a) Illustrations of a parallel, anti-parallel, and hybrid in intramolecular G4 (b) loop conformations of G4.

include NMR analysis, X-ray structural analysis, and CD spectroscopy. Villar-Guerra et al. reported a statistical analysis method using CD spectroscopy (del Villar-Guerra et al., 2018). In this method, the topologies of G4 could be predicted using CD spectroscopy of G4, whose structure is already known. Using these methods, many types of structures were revealed.

Even with the same sequence, some topologies of G4s can be formed. A typical example is G4s in the human telomere (Table 1, Fig. 3) (Phan, 2010). There is a repeat sequence, $(5'\text{-TTAGGG-}3')_n$. This repeat can form G4s and 5′-TTA-3′ is the loop region. Patel et al. first reported the topology of G4 in human telomeres using NMR analysis in the presence of 90 mM Na^+ (PDB ID: 143D) (Fig. 3a) (Wang and Patel, 1993). They found the 22-mer sequence 5′-d[AGGG $(TTAGGG)_3$]-3′ formed an anti-parallel G4. In contrast, X-ray crystal structural analysis revealed that this sequence formed a parallel G4 in 50 mM K^+ (PDB ID: 1KF1) (Fig. 3b) (Parkinson et al., 2002). Furthermore, the hybrid G4 can also be formed by 5′-d[TAGGG $(TTAGGG)_3$ A]-3′ in the presence of 90 mM K^+ as determined via NMR analysis (PDB ID: 2GKU) (Fig. 3c) (Luu et al., 2006). However, other reports used the modified sequence to solve some problems in native sequence analysis, and different topologies were reported in human telomeric sequences (Dai et al., 2007; Matsugami et al., 2007; Phan et al., 2007). According to these reports, despite having the same sequence, topologies of G4 could be different depending on the surrounding conditions, such as metal cations and analysis methods. Since aptamers recognize the targets via their secondary structures, their binding affinity might change if their topologies change. This is the reason why we should take care of the surrounding chemical conditions when we use the G4 aptamers in some applications.

2.2. Conformational change by metal cations

G4 is stable in the presence of cations such as K^+ and Na^+. There are many reports on G4 stability, folding/unfolding and topologies under each metal cation (Bhattacharyya et al., 2016). In this section, we review the examples of various G4 conformations from one sequence in presence of various metal cations. In general, because the cation is located at the center of the G-quartet or between G-quartets, G4s are stabilized (Bhattacharyya et al., 2016). G4 folding/unfolding dramatically changes with or without metal cations, and its conformational change is widely applied to biosensors as the switch of strand displacement (Ma et al., 2017). If the type of metal cation changes, G4 conformations and topologies could be changed depending on the diameter of the metal cation because the distance between G-quartets that coordinate the metal cation might change even with the same sequence. For example, in human telomere, it was reported that the topologies and conformations changed in the presence of different metal cations (Phan, 2010). G4s, which form and stabilize in the presence of the metal cation, can change the conformation because of the addition of other ones. In this section, we will mention recent knowledge about the effects of cations on G4 conformations.

Table 1
Sequences and topologies of G4 in human telomere.

Sequence (5′–3′)	Metal cations	Topology	Method
$AGGG(TTAGGG)_3$	90 mM Na^+	anti-parallel	NMR
$AGGG(TTAGGG)_3$	50 mM K^+	parallel	X-ray
$TAGGG(TTAGGG)_3A$	90 mM K^+	hybrid	NMR

More than two kinds of metal cations competitively bound to the G-quartet and changed the conformation of G4 in some sequences. The conformational change in PW17 (Table 2), competitively bound by Pb^{2+} and K^+ has been reported (Fig. 4) (Yu et al., 2018). Generally, Pb^{2+}-G4 is more stable than K^+-G4, and Pb^{2+} can replace K^+ (Liu et al., 2012). PW17 formed anti-parallel G4-stabilized Pb^{2+} in the presence of 10 μM Pb^{2+}. Under 0.5–10 mM K^+, 10 μM Pb^{2+} could replace K^+ in K^+-stabilized G4 ($2K^+$-PW17) and change its conformation to anti-parallel Pb^{2+}-PW17. The substitution efficiency decreased with increasing K^+ in this range. In contrast, Yu et al. also suggested that K^+ under 10 mM could partly replace Pb^{2+} in stable anti-parallel G4 of Pb^{2+}-PW17 and completely substitute Pb^{2+} at $K^+ > 10$ mM and change its conformation to parallel G4 of $2K^+$-PW17 (Yu et al., 2018). This is different from previous reports that G4 stabilized by Pb^{2+} is more stable than K^+. In addition, they reported that the K^+-Pb^{2+}-PW17 intermediate was formed during the competing process. Ma et al. reported that PW17 formed a stable G4 bound to $1K^+$ and $1Na^+$ ions as the intermediate (Fig. 4) (Ma et al., 2019). Using mass spectroscopy and CD spectrum analysis, they reported that PW17 could form an anti-parallel G4 under a low concentration of Na^+. However, at high concentrations of Na^+, the conformation was changed to the hybrid G4. This conformational change suggests that increasing Na^+ anti-parallel G4 bound to $1Na^+$

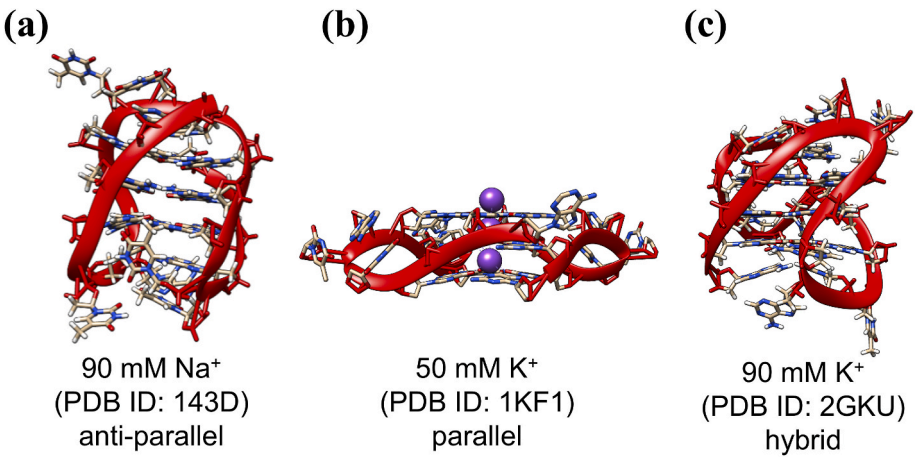

Fig. 3. Structures of human telomeric G4s in the presence of (a) Na^+ by NMR (PDB ID: 143D), (b) K^+ by X-ray crystal structural analysis (PDB ID: 1KF1) and (c) K^+ by NMR analysis (PDB ID: 2GKU).

Table 2
Sequences and conformational changes by metal cations reviewed in the section 2-2.

Name	Sequence (5′–3′)	Metal cation	conformational change
PW17	GGGTAGGGCGGGTTGGG	Pb^{2+} → K^+	anti-parallel to parallel
		Na^+ → K^+	anti-parallel to parallel
		increase of Na^+	anti-parallel to hybrid
T30695	GGGTGGGTGGGTGGGT	Pb^{2+} → Na^+	dimerization of intramolecular parallel G4

changed hybrid G4 bound to $2Na^+$. Furthermore, by adding K^+ to the condition in which PW17 formed hybrid G4 with $2Na^+$, PW17 changed its topology to parallel G4 with $1Na^+$ and $1K^+$, and then parallel G4 bound to $2K^+$.

By changing the concentration and kinds of metal cations, G4s can also promote multimer formation (Fig. 5) (Yu et al., 2016). T30965 (Table 2), which is an aptamer against HIV-1 integrase and forms stable G4 in the presence of Pb^{2+} (Jing et al., 1997). CD spectroscopy revealed that T30695 mainly formed parallel G4 in the presence of 10 μM Pb^{2+} and a small amount of them formed anti-parallel G4. Adding Na^+ to this condition, the peak, indicating anti-parallel G4, disappeared. Therefore, T30695 formed a completely parallel G4 by the addition of Na^+. Further analysis by mass spectroscopy and native polyacrylamide gel electrophoresis (native-PAGE) showed that Pb^{2+} is still bound to T30695 when Na^+ was added. They also analyzed the T30695 mutant, which has two additional thymines at the 5′ or 3′ ends (TT-T30695 and T30695-TT). As a result, only T30695-TT induced dimerization by adding Na^+. Therefore, Na^+ first induced the conformational change in Pb^{2+}-T30695, which was partly parallel to completely parallel. Then, the completely parallel Pb^{2+}-T30695 was dimerized through 5′–5′ stacking. In this case, it was suggested that Pb^{2+} bound between intramolecular G-quartets and Na^+ bound between intermolecular ones.

From these reports, it is suggested that G4, once stabilized by the metal cation, could change its conformation by binding to other kinds of metal cations. When the metal cations competitively bind to G4, they

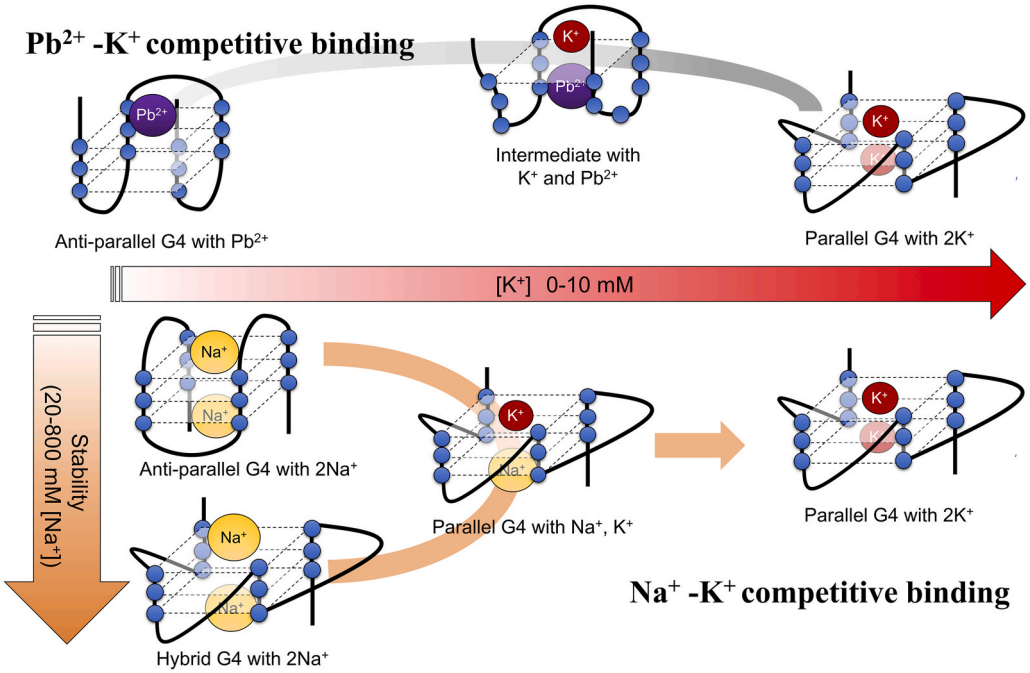

Fig. 4. Illustration of PW17 conformational changes depending on competitive binding of metal cations (Pb^{2+}–K^+ or Na^+-K^+).

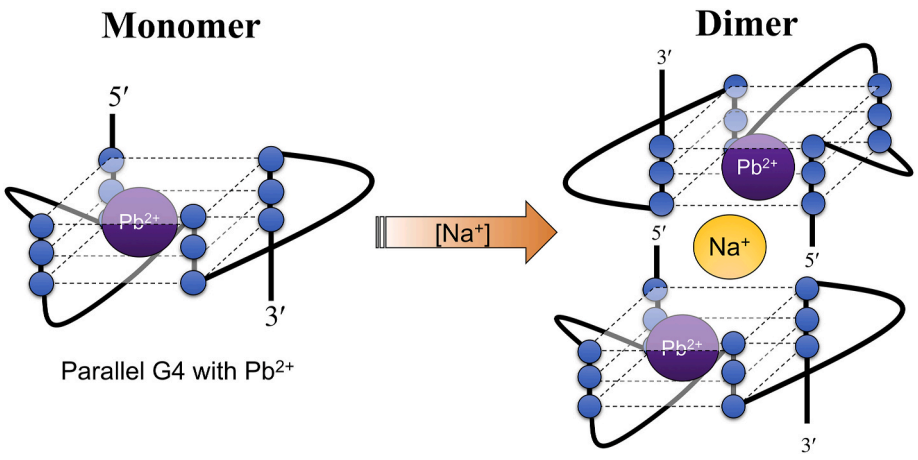

Fig. 5. Conformational changes of Pb^{2+} stabilized G4 in T30695 under the presence of Na^{+}.

can change their topology. Multimer formation was promoted in the presence of two kinds of metal cations, one bound between intramolecular G-quartets and another bound between intermolecular ones. Some studies have suggested that G4 bound by two kinds of metal cations was formed as an intermediate in the competitive binding process. Since the effect of metal cations might be different, it is necessary to investigate many kinds of G4-forming sequences to better understand the effects of cations on G4 conformation. Recently, the G4 folding process in the human telomere, investigated via microscale thermophoresis (MST), was reported (Zhang et al., 2019). In this report, the G4 folding process with K^{+} binding was investigated, and the energetic G4 folding pathway (first G-hairpin was formed then G-triplex was formed) was proposed. Thus, how metal cations affect G4 conformation and folding is gradually being revealed. If more investigations of other sequences and cations are performed by using MST and other methods, we could understand the G4 folding pathway in detail. As mentioned, the types and combinations of metal cations could change G4 conformations (e.g., topology change, multimer formation such as dimerization). These findings are useful for revealing G4 functions *in vivo* as well as in the sequence design of applications such as biosensors. Notably, since the G4 conformation could be changed depending on the kinds and binding orders of metal cations, G4 might be used as an element that can memorize the surrounding environment.

2.3. Conformational change by molecular crowding

Macromolecules, such as proteins, nucleic acids, lipids, and polysaccharides, occupy the intracellular environment. The concentration of these molecules in a cell is reported to be 50–400 g/L (Fulton, 1982). This is approximately 20–40% of cell volume and this crowding condition in cells is believed to play some roles *in vivo*. Since this intracellular environment is much different from the diluted condition *in vitro*, it is necessary to consider that the results *in vitro* could be reproduced in the intracellular environment. This crowding condition indicates not only the intracellular environment but also biological samples, such as serum and blood, measured by biosensors. Therefore, to reproduce the crowding condition *in vivo*, many kinds of co-solutes, such as polyethylene glycol (PEG), have been studied to reveal the function of crowding *in vivo*. Notably, many reports have shown that the conformation and stability of the nucleic acid are much different in crowding conditions compared with diluted conditions (Miyoshi and Sugimoto, 2008). It is suggested that the number of water molecules hydrated to nucleic acids is different among these conditions (Miyoshi et al., 2006). The non-canonical structures of nucleic acids, such as G4, i-motif, and triplex, might have some functions *in vivo* themselves (e.g., transcription, translation, and the maintenance of telomeres) (Brooks et al., 2010; Maizels and Gray, 2013). Therefore, it is necessary to analyze how crowding affects these conformations to reveal their functions *in vivo* (Frank-Kamenetskii et al., 2003; Frank-Kamenetskii and Mirkin, 1995).

The conformations and stability of G4s are dramatically affected by crowding. For instance, the G4 conformations of the telomeric sequences derived from *Oxytricha* (Oxy), *Tetrahymena* (Tet), and humans were reported affected by crowding (Miyoshi et al., 2002, 2005). In human telomeric G4, it has been reported that crowding with PEG changes its conformation, indicating that parallel G4 in the crystal structure is not the main structure in solution (Li et al., 2005). Oxy telomeric sequence forms intramolecular anti-parallel G4 in diluted conditions; however, it forms intermolecular parallel G4 under crowding conditions. Meanwhile, although only one base is different between humans and Tet telomeric sequence, Tet telomeric sequence formed a very long G-wire under the crowding condition; the human sequence did not. Crowding conditions could also affect G4 folding/unfolding. For instance, the telomere DNAs fold into a duplex via Watson-Crick base pairs in diluted conditions. However, they folded into the quadruplex individually, G4 and i-motif, under the crowding conditions (Kan et al., 2006; Miyoshi et al., 2006). From many studies including them, crowding conditions stabilize G4s because of dehydration in general (Petraccone et al., 2012). In this review, since the almost measurement samples of G4-based biosensors containing various metal cations, we provide an overview of the effects of molecular crowding on G4 topologies in the presence of several metal cations.

Zhou et al. reported the evaluation of G4s folded into each topology under crowding conditions with various kinds of metal cations by CD spectroscopy (Table 3) (Zhou et al., 2016). They also evaluated the thermal stability by UV/Vis melting analysis, which could obtain the melting curves from absorbance at 295 nm with temperature gradient. The formation of parallel G4 formed by T30695m and N-Myc did not change in 40% (v/v) PEG with K^{+}, Na^{+}, Sr^{+}, and Ba^{2+}. However, the T_m

Table 3
G4 sequences and conformational changes by crowding conditions in Zhou's and Fujii's reports. (n.d. indicated not detected.)

Topology	Name	Metal cations	Conformational change	Stability
Parallel	T30695m, N-myc	K^{+}, Na^{+}, Sr^{2+}, Ba^{2+}	n.d.	Stabilize
Anti-parallel	HTG	Na^{+}	n.d.	Stabilize
Anti-parallel	HTG	K^{+}	n.d.	Not change
Anti-parallel	TBA	K^{+}	n.d.	Stabilize
Hybrid	HTG	K^{+}	Parallel	–
Hybrid	HTG, JP	Pb^{2+}, Ba^{2+}	n.d.	Destabilize

values of G4 in T30695m in 40% (v/v) PEG with K^+ and Na^+ increased to 32 °C and 25 °C, respectively. N-Myc also improved the thermal stability of G4 in 40% (v/v) PEG with K^+ and Na^+. Therefore, the parallel G4 does not change the conformation but improves the thermal stability in crowding conditions. They evaluated thrombin-binding aptamer (TBA) as a typical anti-parallel G4 model. In TBA, the thermal stability was improved under 40% (v/v) PEG with K^+, whereas it did not change or decrease with bivalent cations. The hybrid G4 were analyzed using the human telomeric G4-forming sequence (HTG). Under 40% (v/v) PEG, the G4 formed in HTG changed the hybrid to the parallel type with K^+.

In contrast, with bivalent cations, such as Ba^{2+} and Pb^{2+}, a conformational change was not observed. However, thermal stability decreased. Therefore, it is assumed that the hybrid G4 is destabilized by crowding conditions. Fujii et al. also reported the properties of anti-parallel G4 under the crowding conditions with Na^+ and K^+ (Table 3) (Fujii et al., 2017). They used an artificial base to control the formation of the Hoogsteen base pairs. In this report, the human telomeric sequence, using modified bases, formed anti-parallel G4. Because of the analysis under different concentrations of PEG200 by UV melting analysis, the thermal stability of the basket-type anti-parallel G4 did not change in the presence of K^+. However, thermal stability improved with Na^+.

Tateishi et al. reported how molecular crowding changes the topologies of G4 using telomeric sequences (Tateishi-Karimata et al., 2020). In this study, the telomeric sequences from humans (Hum) and Tet were analyzed under the various kinds of co-solutes, which are *in vivo* (Fig. 6). They focused on the number of hydroxyl groups in the co-solutes. As mentioned, in the presence of Na^+, the G4 formed in Tet changed its topology from hybrid to parallel under crowding using PEG (Miyoshi et al., 2005). In contrast, Hum formed anti-parallel G4 with or without PEG in the presence of Na^+. CD spectroscopy and native-PAGE showed that Hum did not change their topology under all kinds of co-solutes. Meanwhile, Tet changed its topology and conformation from the intramolecular hybrid G4 to the dimeric form of intermolecular parallel G4, increasing the number of hydroxyl groups in the co-solutes. They calculated the number of water molecules (Nw) located within 3 Å from G4. As a result, the Nw of the anti-parallel G4 in Hum was 326 and that of the parallel was 344. Since dehydration is more stable under crowding conditions, the formation of anti-parallel G4 in Hum is favored. Conversely, the Nw of hybrid G4 in Tet was 337, that of dimer parallel G4 was 324 per a parallel G4. Therefore, the formation of the dimeric parallel G4 was favored under crowding conditions in Tet. In addition, they calculated the Nw of Hum dehydrated by the formation of anti-parallel G4 from single-stranded DNA for each co-solute. Consequently, the Nw decreased as the number of hydroxyl groups in the co-solutes increased. Therefore, the hydroxyl groups in the co-solutes might replace the water molecules surrounding the DNA. They also analyzed other sequences, and hybrid G4s in the diluted condition changed their topologies to intramolecular parallel G4 or dimeric intermolecular parallel G4 under crowding conditions using the co-solute without hydroxyl groups. The parallel G4 in the diluted conditions only changed a monomer to a dimer. Conversely, since some anti-parallel G4s did not change their topologies, others changed the hybrid and parallel G4s; therefore, there is no commonality in the parallel G4s. From these results, co-solutes with one or no hydroxyl groups change the hydration of DNA and induce the formation of parallel G4 (Table 4).

As these studies were performed to characterize G4 conformations by various co-solutes, it seems that G4s had complex conformation characteristics. Effects of crowding on the same sequence could vary depending upon the type of metal cation. In contrast, it might be common that the dimeric intermolecular parallel G4 is more stable than the monomeric one because the number of hydrated water molecules decreased under the crowding condition. Since that dimeric conformation in telomeres is favored as the substrate of the telomerase (Moye et al., 2015), the changes in G4 topology due to the surrounding crowding conditions might have some biological functions. Meanwhile, when we used G4s in some applications such as biosensors, we could easily predict that the results would be different between the experimental and the practical conditions (e.g., blood and serum) because G4 conformations are affected by crowding. Therefore, when we use hybrid or anti-parallel G4s for some applications, it is necessary to investigate how the conformations change under the crowding condition, which mimics the practical samples.

2.4. Conformational change by pH

In vivo, pH changes play many important roles. As the trigger factor of nanoswitches, pH is a good regulator because it can be controlled more easily than other triggers such as protein binding, small molecule binding, and hydration change. The typical structure that changes its conformation by pH is i-motif, which forms in C-rich sequences. In general, i-motifs are stable under a pH range of 4–5 (Day et al., 2014). They have been used in many applications in nanotechnology field, such as pH sensors and drug delivery systems (Alba et al., 2016). In contrast, G4s are destabilized at low pH. However, some sequences could form G4 under neutral pH to low pH. It was reported that a topology change was observed in relation to pH change. In this section, we will review examples of conformational changes due to pH and G4 formation at low pH.

Yan et al. reported that G4 of a specific loop could be transformed based on a corresponding pH change (Yan et al., 2013). They investigated G4 in HTG using CD spectroscopy and NMR. CD spectroscopy revealed that changing pH from 7–4.5 decreased the peak intensity from 290 nm in HTG. Therefore, G4 in HTG changed its conformation in relation to pH. However, this type of transition was not found in other G4-forming sequences *in vivo*, such as RET (Tong et al., 2011), c-myc (Phan et al., 2004), and KRAS (Cogoi and Xodo, 2006). Since the difference between HTG and these sequences is the loop region, they

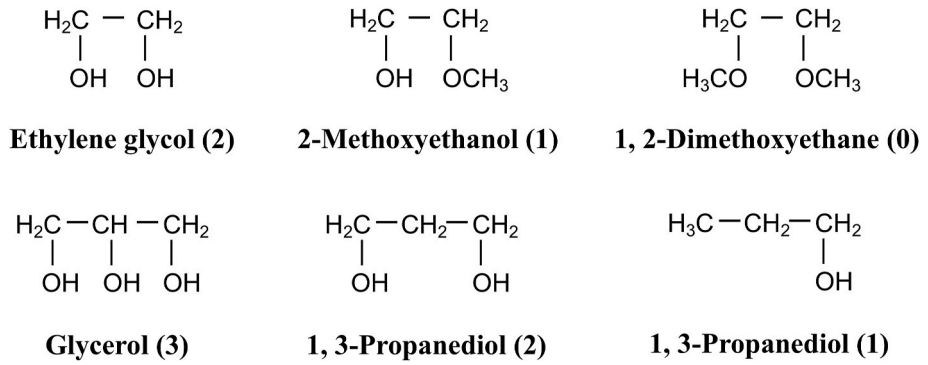

Fig. 6. Co-solutes studied by Tateishi et al. The number of hydroxyl groups was showed inside the parentheses.

Table 4
G4 conformational changes under the various types of co-solutes in Tateishi's report.

Name	Sequence (5′–3′)	Cation	None	Glycerol (3)	1, 2-Dimetoxyethyethane (0)
Tet	$(TTGGGG)_4$	Na^+	Hybrid(monomer)	Hybrid(monomer)	Parallel(monomer, dimer)
Bcl2Mid	GGGCGCGGGAGGAAGGGGGCGGG	Na^+	Hybrid(monomer)	Hybrid(monomer)	Parallel(monomer, dimer)
Hum	$(GGGTTA)_3G_3$	K^+	Hybrid(monomer)	Parallel(monomer, dimer)	Parallel(monomer, dimer)
$d(T_3G_3)_4$	$(TTTGGG)_4$	K^+	Hybrid(monomer)	Parallel(monomer, dimer)	Parallel(monomer, dimer)
Bcl2Mid	GGGCGCGGGAGGAAGGGGGCGGG	K^+	Parallel(monomer, dimer)	Parallel(monomer, dimer)	Parallel(dimer)
Tet	$(TTGGGG)_4$	K^+	Parallel(monomer, dimer)	Parallel(dimer)	Parallel(dimer)
Hum	$(GGGTTA)_3G_3$	Na^+	Anti-parallel(monomer)	Anti-parallel(monomer)	Anti-parallel(monomer)
$d(T_3G_3)_4$	$(TTTGGG)_4$	Na^+	Anti-parallel(monomer)	Anti-parallel(monomer)	Hybrid(monomer)
$d(T_3G_4)_4$	(TTTGGGG)4	Na^+	Anti-parallel(monomer)	Anti-parallel(monomer)	Parallel(monomer)
Oxy	$(TTTTGGGG)_4$	Na^+	Anti-parallel(monomer)	Anti-parallel(monomer)	Parallel(monomer)

investigated HTG variants with various loops. They found that the conformational change resulted from the loop rearrangement. Nevertheless, HTG variants with four and five base central loops did not significantly change their conformation; the variant with TT as the central loop changed its conformation from hybrid G4 to anti-parallel G4 significantly. Furthermore, they found that the conformation changed when the pH decreased due to the rearrangement of the orientation of the loops.

Galer et al. also reported the conformational change of G4 in the human telomeric sequence (Galer et al., 2016). They investigated the sequence htel1-ΔG23, which did not have the 3′-end of guanine. Htel1-ΔG23 formed two types of anti-parallel G4 with two G-quartets, TD and KDH^+ (Fig. 7). These two types of G4 existed in the equilibrium state. TD was the majority in htel1-ΔG23 at neutral pH, and KDH^+ increased when pH decreased. In KDH^+, the unique protonated T18/$A20^+$/G5 base triple and capping base pairs are effectively stacked on a two-quartet core. Since the protonation of A20 was necessary to form KDH^+, htel-ΔG23 changed its conformation with pH change. They also reported that populations of TD and KDH^+ could be controlled by pH. McConnell et al. also reported that G4-forming aptamer, TBA (Bock et al., 1992) with the 5′-end of poly adenines form a hairpin loop structure under low pH (McConnell et al., 2016). TBA has high specificity and affinity for thrombin and has many applications (Avino et al., 2012; Platella et al., 2017). It was suggested that TBA forms G4 at neutral pH and hairpin loop structure at pH 5. This conformational change was caused by the A^+/G base pair, which required the protonation of A to form more stable than a Hoogsteen base pair formed guanines (Lee and Derosa, 2010). Since this A^+/G base pair can only form under lower pH, TBA with the 5′-end of poly adenines can change its conformation. From this report, G4s, which include A in loop regions, could change their conformation by changing pH. Benabou et al. reported the $C{\cdot}C^+$ base pair in the two lateral loops of anti-parallel G4s in the SMARCA4 gene promoter (Benabou et al., 2019). From the results of CD spectroscopy, NMR analysis, and acid-base titrations, the $C{\cdot}C^+$ base pair promoted a reduction in conformational heterogeneity and improved the thermal stability.

The changes in the G4 conformation due to pH were mainly caused by the protonation of A or $C{\cdot}C^+$ base pairing in the loop region. Through the protonation of A, the loop orientations and the patterns of base pairing were changed, and thus G4 might change its conformations.

2.5. Effects of spermine on G4

Spermine is a biogenic polyamine that exists in various types of organisms and tissues. These polyamines play some roles in modulating gene expression and enzyme activities, facilitating DNA-protein interactions, and so on (D'Agostino et al., 2005; Ha et al., 1998). Polyamines are multivalent cations with aliphatic hydrocarbon chains that separate the charges. DNA/RNA backbone phosphate groups interact with the aliphatic hydrocarbon chains that interact electrostatically, and this modulates the structure of DNA/RNA (Thomas and Thomas, 2001). Fu et al. reported that spermine interacts with the G4-forming sequence and induces the formation of microaggregates from an intramolecular parallel G4 (Fu et al., 2011). In contrast, Qi et al. reported that spermine improved G4/hemin enzyme activities (Qi et al., 2014). In this report, the peroxidase activities in various sequences occur with hemins in the presence of spermine. The peroxidase activity of the G4/hemin complex in the intramolecular parallel G4 of PS2.M improved by 6.3-fold in the presence of spermine. Other intramolecular parallel G4s with hemins also improved the peroxidase activities and further analyses were performed using PS2.M as the most improved sequence. Because of CD spectroscopy and UV/Vis spectroscopy, the improvement in activities was caused by the induction of microaggregate formation from the parallel G4. Through this conformational change, a high-activity hemin-binding site between two parallel G4s, which is more hydrophobic, was formed. Since it was also reported that spermine could associate with anti-parallel G4 (Keniry, 2003), spermine might affect G4 conformations, except for the multimerization and microaggregate formations. Other reports suggested that spermine bound to the narrow groove of G4s and attenuated the charge by phosphates (Franceschin et al., 2008; Keniry and Owen, 2013). From these studies, spermine might stabilize G4/hemin complex via attenuating charge and improve its enzyme activity.

3. Applications using G4s

As explained, G4 has the flexibility of changing its conformation in response to surrounding conditions (e.g., metal cations, crowding, and pH). In particular, many biosensors have been reported that use G4 formation to detect metal cations. In this section, we will mainly focus on biosensors and review recently reported applications using the G4 structure itself and their conformational change by surrounding conditions.

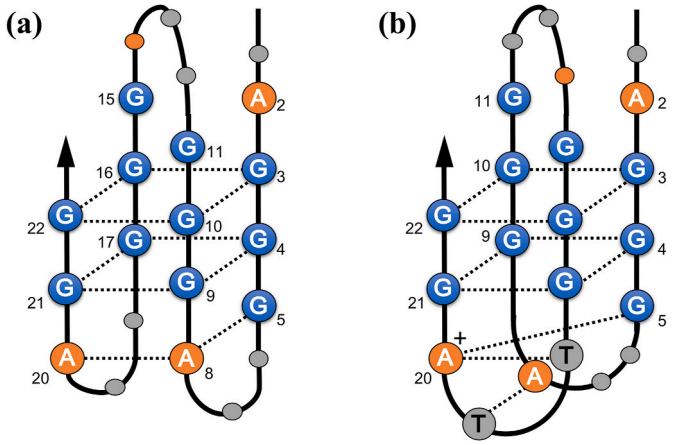

Fig. 7. Two states G4 conformations of htel1-ΔG23 (a) TD, (b) KDH^+.

3.1. Biosensors

3.1.1. Metal cation sensors

The most reported biosensors using G4s are metal cation sensors. There have been some reports on the detection systems of heavy metal cations such as Pb^{2+} and Ba^{2+}, but also the metal cations *in vivo*, such as K^+ (Ji et al., 2019; Xu et al., 2017; Zhang et al., 2016). However, since the binding specificity of metal cations to G4s is not usually sufficient, the main subject of these sensors is how to detect only the target in complex conditions such as polluted water and blood. In this section, we will review recent studies that arranged the design of sequence and the detection principles to achieve specific detection of the metal cation.

Recently, there have been some reports of a cation detection system that can detect the target cation in the presence of other cations. Ye et al. reported a detection system for Ba^{2+} that can work in the presence of K^+ (Fig. 8) (Ye et al., 2019a). In this report, they used G4 in the human telomeric sequence. Through the polarity inversion of the most 3′G in HTG (TAQ-3iG), the G4 conformation changed from natural HTG and improved the binding affinity of Ba^{2+} to G4. TAQ-3iG formed monomeric anti-parallel G4 in the presence of K^+. The polarity inverted G4 tends to favorably dimerize in response to Ba^{2+}. This sensor can detect Ba^{2+} in the presence of 15000-fold excess of K^+ by using hypericin as the fluorescent probe. Yu et al. reported a highly sensitive Pb^{2+} detection system in Na^+-containing samples based on G4 conformational changes. As mentioned, Pb^{2+}-stabilized G4 in T30695 promoted dimerization induced by Na^+ (Yu et al., 2016). They used ZnPPIX as a fluorescence probe and a fully matched ds-DNA containing T30695 as a sensing probe. The presence of Na^+ improves the binding efficiency of Pb^{2+}-stabilized T30695 with ZnPPIX. By using Na^+-induced dimerization of Pb^{2+}-stabilized T30695, they achieved the detection of Pb^{2+} in actual Na^+ containing samples.

These studies improved the specificity of the sensors by improving the binding specificity of G4s with the target metal cation. They achieved the selective detection of each metal cation under the condition, which is close to practical conditions (e.g. including the high concentrations of K^+ or Na^+). The metal cations needed to detect with high selectivity and specificity have almost same radii and dehydration energy (Zhou et al., 2017). Since the binding affinity of metal cations against G4 mainly depend on their radii, they have similar binding affinity to G4. There are limitations to G-quartet patterns and changing the distance between G-quartets by only changing bases in intramolecular G4 sequences, therefore is difficult. The described approaches, polarity inversion and utilization of the target binding to intermolecular G4, could develop the new patterns of G-quartets such as *syn-anti* conformational rearrangements and can be applied to improve the binding selectivity or specificity.

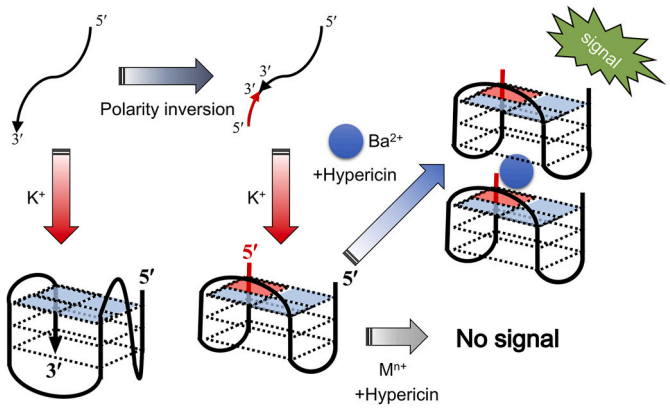

Fig. 8. Scheme of Ba^{2+} detection system by Ye et al.

3.1.2. G4 aptasensors as the recognition element

There are many G4-forming aptamers and applications using them as the recognition element (Roxo et al., 2019). In this section, we will review protein and small-molecule sensors using G4s as the recognition elements. There are many thrombin detection systems using the most studied G4-forming aptamer, TBA (Deng et al., 2014). We also reported the first electrochemical detection system using an aptamer with TBA (Ikebukuro et al., 2004). Here, we focused on recent thrombin detection systems.

Shen et al. reported the ultrasensitive detection system of thrombin by using TBA (Shen et al., 2017). They took advantage of the signal amplification strategy based on chiral supramolecular assembly in the presence of physiological K^+ by a cyanine dye probe DMSB; 3-ethyl-2-[3- (3-ethyl-3H-benzoselenazol-2-ylidene)-2-methylprop-1-enyl] benzoselenazolium bromide. The chiral assembly of DMSB sensitively changes depending on the difference of G4 induced by thrombin and K^+. By combining the unique property of DMSB and TBA with high affinity, they could detect thrombin as low as 2 pM and provided a high selectivity among several interfering compounds such as human serum albumin, immunoglobulin G, lactic acid and so on. They could also detect thrombin with high sensitivity in diluted human serum. Zhang et al. reported the aptasensor of thrombin, which can be photo-driven and regenerated (Zhang et al., 2020). They modified TBA by inserting five azobenzenes. This sensor can be regenerated by ultraviolet light exposure since the azobenzene structure is transformed from *trans* to *cis* and opens the folded TBA. This system can detect a linear thrombin concentration from 5 pM to 5 μM. By introducing modifications, they overcame one of the critical challenges of aptasensors, their regeneration. AS1411 is a G4-forming aptamer against nucleolin, which is overexpressed on surface of cancer cells (Bates et al., 2009). Feng et al. reported the electrochemical aptasensor of label-free cancer cell detection by using AS1411 (Feng et al., 2011). They could detect as low as one thousand cancer cells such as HeLa, K562, and NIH3T3 with high selectivity. This aptasensor can be regenerate using complementary strand of AS1411 and can be reused for cancer cell detection. Gao et al. reported a connective tissue growth factor (CTGF) detection system using a CTGF-binding aptamer (Gao et al., 2019). They obtained a CTGF-binding aptamer, APT1, which formed interconvertible parallel and anti-parallel G4, and improved them by introducing mutations and truncating. APT1M6T was obtained as a result of improvements, which formed an anti-parallel G4 with a higher affinity than APT1. They also introduced a locked nucleic acid sequence to APTM6T and developed a BLI-based enzyme-linked aptamer sandwich assay of CTGF with a wide detection range from 0.05–50 nM.

There are also G4 aptasensors for small molecules. The adenosine triphosphate (ATP) binding aptamer folds into G4 when it binds to ATP (Huizenga and Szostak, 1995). There were some reports of the ATP aptasensor using Thioflavin T (ThT) as a fluorescence indicator (Ji et al., 2017; Liu et al., 2017). These aptasensors could detect ATP with high sensitivity (a detection limit with 18 nM (Liu et al., 2017), 33 nM (Ji et al., 2017) each) in around 10 min. Qi et al. reported the detection of zeatin, which is a cytokinin regulates a various processes in plants with high selectivity (Qi et al., 2013). They developed the fluorescence turn-on aptasensor using graphene oxide and fluorescence-labeled G4-forming aptamer, which obtained the linear range from 3 to 50 μM and its limit of the detection was 0.1 μM.

Since G4-forming aptamers have various targets from small molecules to proteins, the aptasensors based on them have been developed against various targets including cancer cells. These studies suggested that introducing modifications to G4-forming aptamers could improve the aptasensors with desirable characteristics such as photo-driven regeneration and achieve the wide detection range of aptasensors by improving binding affinity of aptamers.

3.1.3. G4s as the signal elements

There are many reports of the use of G4s as signal elements. There

are two main types of signal elements based on G4s: derived from DNAzyme activity and from G4-specific ligands. G4/hemin complex works as DNAzyme, which has peroxidase activity and is applied to various biosensors (Kosman and Juskowiak, 2011). Various types of G4-specific ligands have been developed and applied as the fluorescence signal generators (Umar et al., 2019). There is the exception of these signal elements based on G4, Spinach that is G4-forming RNA aptamer against the DFHBI and generates fluorescence only upon binding to it (Paige et al., 2011). In this section, we introduce the recent biosensors using G4s as the signal elements such as peroxidase activity, fluorescence, and the electrochemical signal of a G4 specific ligand.

Many Pb^{2+} detection systems that used the G4/hemin complex as a signal element, not G4s as the recognition element, have been reported (Liang et al., 2017). Ji et al. reported that the Pb^{2+} sensor used G4/hemin complex to enhance its signal (Fig. 9a) (Ji et al., 2019). They used a Pb^{2+}-specific DNAzyme, the 8–17 DNAzyme, consisting of the enzyme strand (ES) and the substrate strand (SS) (Brown et al., 2003). In the presence of Pb^{2+}, the SS is cleaved and the ES is exposed as a single stranded DNA. Then, the helper DNA which is a complementary strand of ES is hybridized with the ES. The helper DNA has a G-rich sequence that forms G4 as the signal element. When hemin is added to them, G4/hemin complexes are formed, and we can measure the current because of MoS2–AuPt nanocomposites and G4/hemin cocatalyze the reduction of H_2O_2. This signal enhancement achieved a high sensitivity for this sensor, which can detect Pb^{2+} from 0.1 pg/mL to 1000 ng/mL with a limit of detection of 38 fg/mL. There have also been reports of sensors using the G4/hemin complex as the signal-generating element. Wang et al. reported an ochratoxin A (OTA) sensor using the G4-triplex ligand (Fig. 9b) (Wang et al., 2019). OTA is a typical mycotoxin that causes nephrotoxicity, embryotoxicity, hepatotoxicity, and immunotoxicity *in vivo* (Pfohl-Leszkowicz and Manderville, 2007). OTA is a typical mycotoxin that causes nephrotoxicity, embryotoxicity, hepatotoxicity, and immunotoxicity *in vivo* (Cruz-Aguado and Penner, 2008). They designed a triple helix aptamer probe (TAP) in which each end of the OTA binding aptamer was modified to form a triple helix with the G4-forming probe. In the absence of OTA, TAP forms the triple helix, which has the OTA binding aptamer as the loop. In contrast, the aptamer binds to OTA and collapses the triple-helix structure of TAP in the presence of OTA, releasing the G4-forming probe. To form G4 in the released probe, K^+ and hemin were added. The signal from the G4/hemin enzyme activity was detected via chemiluminescence using the luminol-H_2O_2 system. Because the signal probe is released only by OTA binding to the aptamer, they achieved a low background signal. This sensor can detect OTA in the range of 0.1–2.0 ng/mL with a linear dependence, and the limit of detection was 0.07 ng/mL. Furthermore, this sensor can detect OTA with high selectivity because of its specificity with the OTA binding aptamer. They measured the spiked OTA in wine with 92–99% accuracy using this sensor.

G4-specific ligands that generate fluorescence signal only when binding to G4s are also used widely in biosensors (Bader and Cockroft, 2018). They are also applied to monitoring and imaging G4s in living cells. For instance, Xu et al. developed a technique cyanine dye called CyT to detect various types of RNA G4s from *in vitro* to living human cells (Xu et al., 2015). The G4-specific ligand called IMT was developed for real-time visualization of DNA G4s in living cells (Zhang et al., 2018). As mentioned in section 3-1-1 and 3-1-2, some G4-based aptasensors were designed with both the properties of G4, target recognition and signal generation, such as the Ba^{2+} detection system (Ye et al., 2019b) and ATP detection systems (Ji et al., 2017; Liu et al., 2017). G4-specific ligands have been applied to these systems (Roxo et al., 2019; Xi et al., 2020; Yang et al., 2020). On the other hand, there is a study reporting that G4-forming probe and G4-specific ligand is applied as only the signal generator. Dai et al. reported a detection system for both melamine and iodide using one G4-forming probe (Fig. 10) (Dai et al., 2019). They designed a probe that formed G4 in the presence of melamine or iodides. The signal is detected as fluorescence by binding N-methyl mesoporphyrin IX (NMM), which is a parallel G4 specific fluorescent ligand (Nicoludis et al., 2012). In the detection of melamine, the designed probe is a single-stranded DNA in the absence of melamine. By adding K^+ and NMM to this, the probe forms G4, and NMM binds to it, allowing the fluorescence signal to be detected. In contrast, in the presence of melamine, melamine intercalated with five thymine bases at both ends of the probe. Therefore, G4s are not formed, which indicates no signals. To detect iodides, they use Hg^{2+}, which interacts with the probe in the

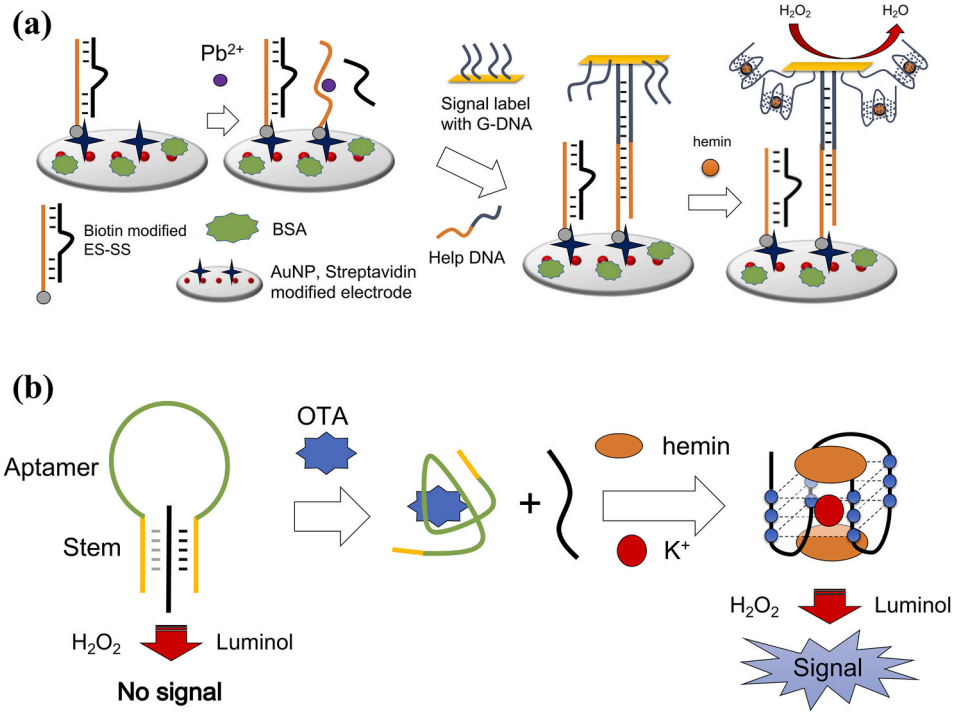

Fig. 9. Scheme of detection systems using G4/hemin as signal elements (a) Pb^{2+} detection by Ji et al., (b) OTA detection system by Wang et al.

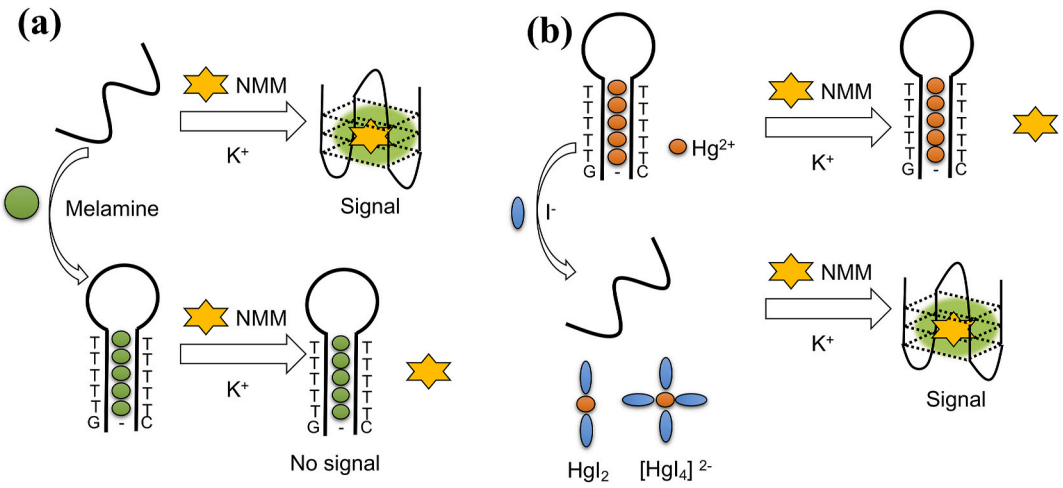

Fig. 10. Scheme of melamine (a) and iodide (b) detection system by Dai et al.

same manner as melamine, and the probe forms the stem-loop structure. In the presence of iodides, Hg^{2+} was released from thymine bases because they interacted with iodides (forming HgI_2 and $[HgI_4]^{2-}$). By adding NMM and K^+ to this condition, G4s were formed by the probes and the signal can be detected as fluorescence. In the absence of iodides, G4s were not formed by adding NMM and K^+ since Hg^{2+} was not release from thymine bases. In other words, the fluorescence signal decreased depending on the amount of melamine, while it increased depending on that of iodides. The limits of detections were 0.08 nM and 4.6 nM for melamine and iodide, respectively. They also reported that this sensor had high selectivity against other factors in real samples. Spinach, the RNA aptamer binds to the fluorophore (DFHBI) briefly described in section 1, has been applied to detect a variety of molecules *in vitro* and perform living cell imaging of them. Paige et al., who developed Spinach aptamer, fused the aptamers against small molecules such as adenosine, adenosine 5′-diphosphate (ADP), S-adenosylmethionine (SAM), guanine and guanosine 5′-triphosphate to Spinach via its loop region (Paige et al., 2012). These modified RNA sensors were activated and the fluorescence was switched on only when their target binding occurred in the presence of DFHBI. The fluorescence increases corresponding on the target binding were linear in physiological concentration ranges. Especially they suggested that the SAM and ADP sensor could be applied to monitor metabolite dynamics in living cells by using DFHBI-treated *Escherichia coli* expressing each RNA sensor. There are many reports about Spinach applied to biosensors against not only small molecules (Dasgupta et al., 2015; Nakayama et al., 2012) but proteins such as streptavidin, MS2 coat protein and thrombin (Song et al., 2013); mRNA (Guet et al., 2015; Ong et al., 2017; Zhang et al., 2015) and miRNA (Aw et al., 2016; Ying et al, 2017, 2018). Since Spinach is RNA, it could be expressed in cells and applied to imaging and monitoring the molecules *in vivo*.

Tang et al. reported the sensitive sensor of micro RNA (miRNA) by measuring electrochemical signals by forming G4s triggered from strand displacements (Tang et al., 2020). In the presence of the target miRNA, the probe is released by the toehold-mediated strand displacement reaction (TMSDR). This probe includes the sequence of the complementary strand of ssDNA on the electrode and C-rich sequence, which is the complementary strand of RCA templates. The RCA reactions are performed using the released probe and the long G4-forming probes are synthesized. After the reaction, this long probe is immobilized to the electrode via single-stranded DNA. Then, methylene blue (MB) and K^+ are added, and MBs bind to G4s. Finally, the target miRNA can be detected by measuring the current by reducing the MB. The limit of detection in this sensor is 2.75 fM, and this sensor can detect the miRNA with higher reproducibility than RT-PCR. Furthermore, this sensor achieved high selectivity because of the trigger of reactions based on the strand displacement.

3.2. Other applications using G4s

G4s are used in other applications because of their flexible conformations. In this section, we review recent applications, except biosensors.

3.2.1. The molecular crowding sensor

The conformational change in G4 driven by crowding conditions was also applied to analyze the intracellular crowding condition. Sugimoto et al. used a human telomeric sequence in this system (Takahashi et al., 2019). They used a hairpin DNA-human telomeric G4 conjugate sequence. The human telomeric G4 changed its conformation under crowding conditions (Miyoshi et al., 2002). For example, anti-parallel G4 was formed in the presence of Na^+, mixed, hybrid in the presence of K^+, and parallel G4 in the presence of K^+ under crowding conditions. The hairpin was conjugated to the end of the 5′ human telomeric G4 and Cy5 was modified to the third base position of HP. Cy3 was attached to the 3′ terminus of human telomeric G4. In this system, the difference in Förster resonance energy transfer (FRET) efficiency among the G4 topologies was detected. They analyzed HeLa cells using this sensing system and detected differences in crowding between the cytosol and nucleus and suggested that the nucleus was more crowded than the cytosol. Furthermore, some spots observed in the nucleus with high FRET efficiency corresponded to membrane less organelles such as the nucleolus. The crowding environment in cells might vary according to the region of the cell. This is the only report that conformational changes in G4 by crowding were applied to the sensing system.

3.2.2. pH responsive applications

Although i-motifs are the most applied structure that changes their conformation in relation to pH (Alba et al., 2016), some applications use the conformational change in G4 by pH variation. McConnell et al. reported a protein release system responding to pH using TBA with a modified sequence (McConnell et al., 2016). TBA binds to thrombin at a neutral pH by forming G4. When pH decreased (e.g., pH 5), thrombin was released because the conformation of the modified TBA changed from anti-parallel G4 to a hairpin loop structure. Yan et al. also reported that G4 conformational changes due to pH variation could be applied in a nanoswitch (Yan et al., 2013). They reported that G4 derived from the human telomeric sequence could be applied as a pH-driven nanoswitch with three gears. Thiazole orange (TO) is used as a fluorescent probe that specifically binds to G4s (Lubitz et al., 2010). There was a difference in

the fluorescence intensity of the TO-G4 complex between pH7 and pH4.5. As mentioned, this sequence formed a different type of G4, hybrid in pH7, and parallel in pH4.5. Therefore, they concluded that the difference in fluorescence intensity was caused by conformation change-driven pH variation. The kinetic process of G4 conformation change by pH variation was much slower than that of i-motif. Furthermore, the repeatability of the G4 conformation change was worse than that of the i-motif after a few cycles. However, G4 could form one more folding conformation and establish a system with three gears. Since there have been more studies using i-motifs and triplexes as the pH-responsive element than G4s (Bielecka et al, 2015, 2019; Chandrasekaran and Rusling, 2018; Hu et al., 2017), further analysis and investigations using G4s are needed to determine which conformation is the best element.

3.2.3. *Drug delivery system*

There are some reports of protein/drug delivery systems using G4s. Carvalho et al. reported a ligand delivery system for cancer cells using a G4-forming aptamer (Carvalho et al., 2019). They applied the nucleolin-binding aptamer, AS1411 (Bates et al., 2009) to deliver an acridine-based G4 ligand, C_8, to HeLa cancer cells. This method reduced the cytotoxicity of the ligand compared to non-malignant cells because the ligands were specifically delivered into cancer cells via nucleolin and aptamer binding. Yang et al. also reported a drug delivery system using AS1411 for enhanced photodynamic therapy (PDT) (Yang et al., 2018). They developed a DNA nanostructure consisting of AS1411, achlorine e6 (Ce6) as a drug, Ca^{2+} to form nanostructures, and hemin. This method also used AS1411 as the carrier drug in cancer cells. Furthermore, the generation of oxygen *in situ* from H_2O_2 by G4/hemin DNAzyme activity enhanced PDT because the hypoxia-associated resistance was reduced.

3.2.4. *Metal cation transporter on a biomimetic membrane*

Li et al. applied lipophilic G4 as biomimetic ion channels (Li et al, 2019, 2020). First, they reported K^+ transporters using a sequence that forms parallel G4 in the presence of K^+ (Cheng et al., 2016). They then reported the K^+-Pb^{2+} selective transporter, PS2.M (Fig. 11). To overcome the transport selectivity of the biomimetic membrane, they modified the PS2.M sequence to fold into anti-parallel and parallel G4. For these applications as membrane transporters, they modified the sequence by adding some lipophilic 12-carbon spacers and a cholesterol moiety as the hydrophobic domains. In the latter report, Pb^{2+}-stabilized G4 and K^+-stabilized G4 can transport Pb^{2+} and K^+, respectively, with high selectivity (Pb^{2+}/K^+ selectivity = 30.6, K^+/Pb^{2+} selectivity = 31.8). They reported that G4-mediated transport is dependent on the G4 coordination of metal cations.

4. Developments of G4 sequence for applications

As mentioned above, there are various applications using G4s. Some approaches have been used to develop more practical applications, topology-specific G4 ligands (Ma et al., 2020) and modifications by artificial nucleic acids (Gao et al., 2019). In this section, we review the recent approaches used to improve and design G4 sequences for applications, except the introduction of artificial nucleic acids, as mentioned in section 3.

G4-specific ligands could be also applied to control the conformation of aptamers. We previously reported that the G4-specific ligand, L1H1-7OTD stabilized the folded structure of G4-forming aptamers and enhanced their binding properties (Tsukakoshi et al., 2016). This study suggested that G4-specific ligands could be applied to the aptasensors based on G4 by improving the binding ability of the aptamers.

Wang et al. developed a metal-cation-free G4/hemin DNAzyme in the S1 nuclease detection system (Wang et al., 2016). In general, metal cations are necessary to form parallel G4, which has DNAzyme activity. They directly modified hemin to the 5′ ends of a G4-forming sequence (G4-hemin). G4-hemin spontaneously split into G4 and hemin and had higher peroxidase activity than the non-modified G4/hemin complex.

Other approaches have reported the investigation and design of split G4 probes for more selective applications. Lv et al. explored the intramolecular split of G4, which formed in a spacer-inserted G4-forming sequence, using T30695 as a typical G4 (Lv et al., 2019). They investigated the length and location of the spacer sequence (Fig. 12). Although the intramolecular split G4 they studied can fold into G4, however, the thermodynamic stabilities were different. For instance, non-classical intramolecular split G4s had lower stability than the classical ones. Connelly et al. proposed the rational design of an intermolecular split G4 peroxidase-like DNAzyme (sPDz) probe that provides a visual output signal (Connelly et al., 2019). The sPDz probe consists of two strands with target recognition sequences that are hybridized to the target site and folded into G4, which catalyzes H_2O_2-mediated oxidations in the presence of heme. They investigated the effects of the numbers of C and single nucleotide substitutions (SNSs) in target sequences on the signal

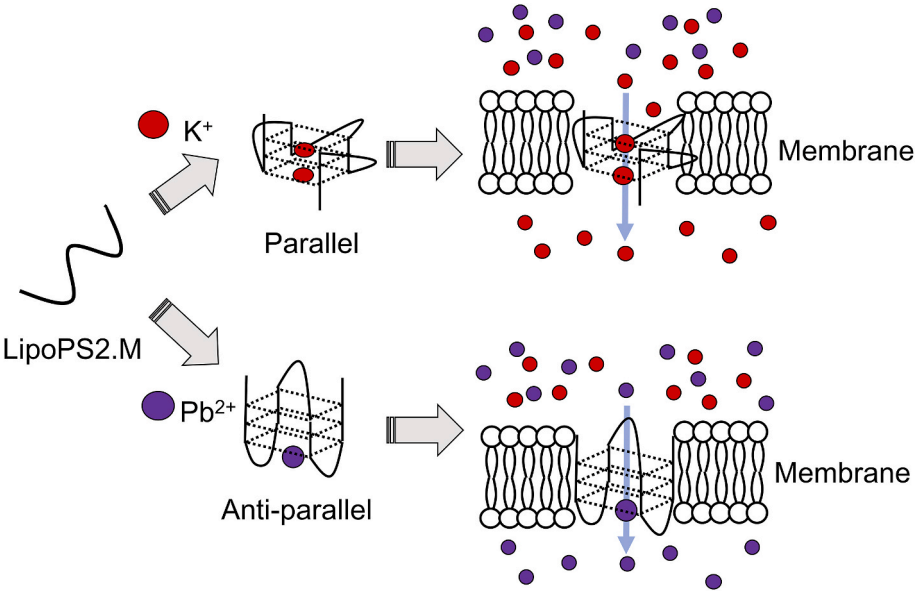

Fig. 11. Illustrations of G4 as a K^+-Pb^{2+} transporter on biomimetic membranes.

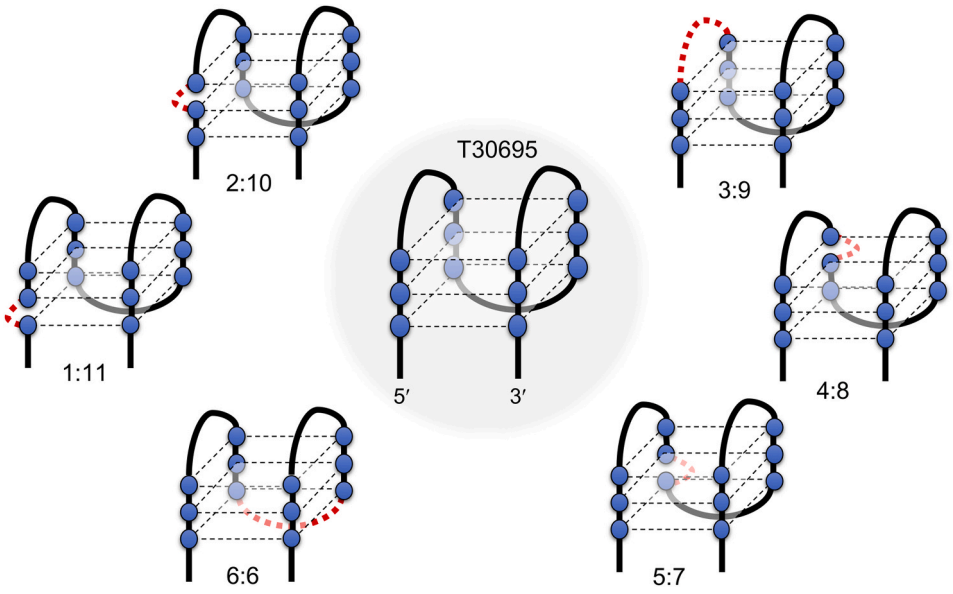

Fig. 12. Illustrations of intramolecular split G4 conformations studied by Lv et al.

turn-on ratio, and proposed strategies to overcome some challenges such as high background, decreased signals, and no SNS discrimination.

As mentioned in 3-1-1, a polarity inversion is one of the effective approaches to regulate and improve G4 probes for desirable functions. Smirnov et al. reported a series of three-layer intramolecular G4s, including forward or reverse G-tracts, by non-natural or thymine loops (Smirnov et al., 2020). They characterized G4 foldings and conformations using spectroscopic and electrophoretic methods. They used tetraethyleneglycol (L) to invert the polarity. From the results of the comprehensive analysis using muted G4 sequences, the loop type and location, the G-strand arrangement contributed to the G4 folding topology, structural polymorphism, dimerization, and stability. For instance, the non-natural G4s, including L-loops showed the dimerization and building of 5′/5′ interface might be an independent driver of parallel folding. Various conformations and topologies of G4 with polarity inversion than natural ones could be used for applications to achieve high specificity and sensitivity.

5. Summary and conclusions

In this review, we summarized how the surrounding conditions of the environment, such as metal cations, pH, and crowding affected G4 conformations and their applications as well as recent studies on the design of G4-forming sequences. The most investigated factor that changes G4 conformation is metal cations. In general, monovalent or bivalent cations stabilizes G4 formation by binding to the G-quartet. Each cation has a different binding affinity to G4, forming oligonucleotides, and some cations competitively bind to them. Recently, there have been reports on how two kinds of cations competitively bind to G4 and affect its conformation. The replacement of cations in the intramolecular G-quartet could change its topology. PW17 changed parallel G4 from hybrid G4 because Na^+ in the intramolecular G-quartet was replaced by K^+, for instance. In contrast, some types of cations did not bind to G4 competitively. In this review, we found that Na^+ or K^+ promoted the dimerization of G4 stabilized by Pb^{2+} or Ba^{2+}. These conformational changes were caused by the difference in each cation-binding pattern; one bound to intramolecular G-quartet and the other to intermolecular. Using this knowledge, some cation detection systems have been reported with high selectivity and sensitivity achieved by using the conformational change in G4.

Some reports have investigated the effects of pH variation. Some kinds of sequences changed conformation driven by changes in pH. There were some reports that the protonation of A in the loop region was the trigger of conformation change. When adenine was protonated at low pH, a $A^+ \cdot G$ base pair was formed. Because of this base pairing, the orientations of loops could be changed, and the conformation such as topologies could be changed. The responses of G4 to pH variation were different among sequences, especially loop regions. However, this conformational change is almost reversible because it is caused by the changing protonation. Therefore, the ability of G4 to respond to pH changes and change its conformation could be applied to nanoswitches such as protein delivery systems.

The effects of crowding conditions on G4 were investigated mainly using co-solutes such as PEG. Since the hydration and dehydration states were changed by crowding, the conformation and thermal stability of G4 were changed. A topology-based study was conducted, which suggested that parallel G4 is stabilized under crowding conditions. Other topologies, such as anti-parallel and hybrid G4s, were suggested to show various effects by crowding conditions in the presence of different cations. It is very complicated how the crowding effects on G4 are different among sequences and the coexistence of cations. However, a crowding sensing system was developed *in vivo* using G4-forming oligonucleotides. If it is revealed how the crowding effects on G4 conformations and other applications could be developed, then the function of G4 *in vivo* might be clarified.

We also summarized applications using G4, with a special focus on biosensors. We showed the characteristics of G4-based biosensors described in this review on Table 5. G4s were widely applied as both recognition and signal elements such as metal cation and thrombin sensors. Some studies overcame the low selectivity of G4-based metal cation sensors by polarity inversion and binding the target to intermolecular G4. These studies characterized the G4s in the conditions required to reproduce the practical sample (e.g. abundance of K^+ and Na^+). By modifying G4-forming sequence with artificial nucleic acids or using the complementary strand, some G4 aptasensors could be reused and achieved high sensitivity and selectivity. G4/hemin complex and G4-specific ligands have been widely used and improved as the signal elements. By combining these approaches to improve G4-based biosensors, it could be achieved to practically use them for diagnosis, environmental measurement and so on.

In almost all the applications, they should be applied to real samples such as blood and polluted water. The environmental responsive properties of G4 are advantageous for detecting changes in the surrounding conditions. However, they are also disadvantageous to the

Table 5
The summary of the features of G4-based biosensors described in this review.

Feature	Advantage	Disadvantage	Approaches for disadvantage	Reference
Metal cation sensor	High sensitivity	Low selectivity	Polarity inversion(high selectivity and K^+ tolerance)	Ye et al. (2019)
			Applying binding Pb^{2+} to intermolecular G4(high selectivity and Na^+ tolerance)	Yu et al. (2016)
G4 aptasensor	High affinity, high sensitivity	Disturbed G4 folding by K^+	Applying the sensitive ligand against the G4 changes induced by K^+ and thrombin(Improve sensitivity, K^+ tolerance)	Shen et al. (2017)
		Single-use	Inserting azobenzenes to regenerate sensors by UV	Zhang et al. (2020)
			Applying the complementary strand for regeneration	(Feng et al., 2011)
		Low nuclease resistance	Introducing LNA to the aptamer(Improve thermal stability, nuclease resistance)	Gao et al. (2019)
		Need to label aptamers	Applying G4-specific ligand with high specificity (Improve sensitivity, rapid detection)	Ji et al. (2017), Liu et al. (2017)
		Need more affinity	Applying G4-specific ligand with high specificity (Improve binding ability.)	Tsukakoshi et al. (2016)
G4/hemin complex	Various kinds of signals Use for signal amplification	Necessary of metal cation	Directly modify hemin to G4-forming sequence(DNAzyme activity without metal cations is achieved)	Wang et al. (2016)
G4-specific ligand	Label-free	Some background	Improve G4-specific ligands themselves	Xu et al. (2015), Zhang et al. (2018)
			Design the sequence and select proper ligands	Dai et al. (2019)

reproducibility of the G4-forming aptamer bindings. To overcome these disadvantages, it is necessary to reveal the factors that change and affect G4 conformations. If they were revealed, we can improve the measurement conditions or decide on the range of applications depending on the sample conditions and might achieve the detection with high reproducibility. As mentioned, some approaches to the G4-forming sequence were performed, such as introducing artificial nucleic acids and inverting the polarity. Using these methods, we can provide new properties (e.g., high stability, selectivity, and sensitivity) that natural G4s do not have.

6. Future perspective

To apply G4 on various systems and understand its functions *in vivo*, further analyses are needed. Recently, analytical methods, such as microscale thermophoresis, which can simultaneously detect ion binding and structural change, were used for the characterization of the G4 conformation (Zhang et al., 2019).

Thus, the folding pathways of G4 in some common sequences (e.g., human telomeric sequence) were gradually dissected out. These findings are helpful for the design and improvement in the G4-forming sequence for favorable applications. However, more types of G4s should be analyzed because the responses to varying conditions are different among sequences. If more types of G4s are characterized, we could get deeper insights to understand G4 functions *in vivo* and design sequences for desirable applications. As mentioned, the optimization of the conditions and the decision on the range of G4 applications should be necessary for practical use. Nevertheless, there are many G4-forming aptamers with high affinity; only some of them have been characterized in terms of the environmental responsivity. If these aptamers were characterized and improved, the possibility of applications that use G4 might expand to a wide field.

Declaration of competing interest

The authors declare that they have no known competing financial interests or personal relationships that could have appeared to influence the work reported in this paper.

Acknowledgements

This work was supported by the JST-Mirai Program Grant Number JP19216403, Japan.

References

Adrian, M., Heddi, B., Phan, A.T., 2012. NMR spectroscopy of G-quadruplexes. Methods 57, 11–24. https://doi.org/10.1016/j.ymeth.2012.05.003.
Alba, J.J., Sadurní, A., Gargallo, R., 2016. Nucleic acid i-motif structures in analytical chemistry. Crit. Rev. Anal. Chem. 46, 443–454. https://doi.org/10.1080/10408347.2016.1143347.
Alberti, P., Mergny, J.-L., 2003. DNA duplex–quadruplex exchange as the basis for a nanomolecular machine. Proc. Natl. Acad. Sci. Unit. States Am. 100, 1569–1573. https://doi.org/10.1073/PNAS.0335459100.
Avino, A., Fabrega, C., Tintore, M., Eritja, R., 2012. Thrombin binding aptamer, more than a simple aptamer: chemically modified derivatives and biomedical applications. Curr. Pharmaceut. Des. 18, 2036–2047. https://doi.org/10.2174/138161212799958387.
Aw, S.S., Tang, M.X., Teo, Y.N., Cohen, S.M., 2016. A conformation-induced fluorescence method for microRNA detection. Nucleic Acids Res. 44, 1–9. https://doi.org/10.1093/nar/gkw108.
Bader, A., Cockroft, S.L., 2018. Simultaneous G-quadruplex DNA logic. Chemistry 24, 4820–4824. https://doi.org/10.1002/chem.201800756.
Bates, P.J., Laber, D.A., Miller, D.M., Thomas, S.D., Trent, J.O., 2009. Discovery and development of the G-rich oligonucleotide AS1411 as a novel treatment for cancer. Exp. Mol. Pathol. 86, 151–164. https://doi.org/10.1016/j.yexmp.2009.01.004.
Benabou, S., Mazzini, S., Aviñó, A., Eritja, R., Gargallo, R., 2019. A pH-dependent bolt involving cytosine bases located in the lateral loops of antiparallel G-quadruplex structures within the SMARCA4 gene promotor. Sci. Rep. 9, 1–16. https://doi.org/10.1038/s41598-019-52311-5.
Bhattacharyya, D., Arachchilage, G.M., Basu, S., 2016. Metal cations in G-quadruplex folding and stability. Front. Chem. 4, 1–14. https://doi.org/10.3389/fchem.2016.00038.
Bielecka, P., Dembska, A., Juskowiak, B., 2019. Monitoring of pH using an i-motif-forming sequence containing a fluorescent cytosine analogue. TC. Molecules 24. https://doi.org/10.3390/molecules24050952.
Bielecka, P., Juskowiak, B., Jacques, J., Eynde, V., 2015. Fluorescent sensor for PH monitoring based on an i-motif- – switching aptamer containing a tricyclic cytosine analogue (tC), 18511–18525. https://doi.org/10.3390/molecules201018511.
Bock, L.C., Griffin, L.C., Latham, J.A., Vermaas, E.H., Toole, J.J., 1992. Selection of single-stranded DNA molecules that bind and inhibit human thrombin. Nature 355, 564–566. https://doi.org/10.1038/355564a0.
Brooks, T.A., Hurley, L.H., 2009. The role of supercoiling in transcriptional control of MYC and its importance in molecular therapeutics. Nat. Rev. Canc. 9, 849–861. https://doi.org/10.1038/nrc2733.
Brooks, T.A., Kendrick, S., Hurley, L., 2010. Making sense of G-quadruplex and i-motif functions in oncogene promoters. FEBS J. 277, 3459–3469. https://doi.org/10.1111/j.1742-4658.2010.07759.x.
Brown, A.K., Li, J., Pavot, C.M., Lu, Y., 2003. A lead-dependent DNAzyme with a two-step mechanism †, 7152–7161. https://doi.org/10.1021/bi027332w.
Burch, B.D., Garrido, C., Margolis, D.M., 2017. Detection of human immunodeficiency virus RNAs in living cells using Spinach RNA aptamers. Virus Res. 228, 141–146. https://doi.org/10.1016/j.virusres.2016.11.031.
Carvalho, J., Paiva, A., Cabral Campello, M.P., Paulo, A., Mergny, J.L., Salgado, G.F., Queiroz, J.A., Cruz, C., 2019. Aptamer-based targeted delivery of a G-quadruplex ligand in cervical cancer cells. Sci. Rep. 9, 1–12. https://doi.org/10.1038/s41598-019-44388-9.

Chambers, V.S., Marsico, G., Boutell, J.M., Di Antonio, M., Smith, G.P., Balasubramanian, S., 2015. High-throughput sequencing of DNA G-quadruplex structures in the human genome. Nat. Biotechnol. 33, 877–881. https://doi.org/10.1038/nbt.3295.

Chandrasekaran, A.R., Rusling, D.A., 2018. Triplex-forming oligonucleotides : a third strand for DNA nanotechnology, 46, 1021–1037. https://doi.org/10.1093/nar/gkx1230.

Chen, F.M., 1992. Sr2+ facilitates intermolecular G-quadruplex formation of telomeric sequences. Biochemistry 31, 3769–3776. https://doi.org/10.1021/bi00130a006.

Cheng, H., Qiu, X., Zhao, X., Meng, W., Huo, D., Wei, H., 2016. Functional nucleic acid probe for parallel monitoring K+ and protoporphyrin IX in living organisms. Anal. Chem. 88, 2937–2943. https://doi.org/10.1021/acs.analchem.5b04936.

Cogoi, S., Xodo, L.E., 2006. G-quadruplex formation within the promoter of the KRAS proto-oncogene and its effect on transcription. Nucleic Acids Res. 34, 2536–2549. https://doi.org/10.1093/nar/gkl286.

Connelly, R.P., Verduzco, C., Farnell, S., Yishay, T., Gerasimova, Y.V., 2019. Toward a rational approach to design split G-quadruplex probes. ACS Chem. Biol. 14, 2701–2712. https://doi.org/10.1021/acschembio.9b00634.

Cruz-Aguado, J.A., Penner, G., 2008. Determination of ochratoxin A with a DNA aptamer. J. Agric. Food Chem. 56, 10456–10461. https://doi.org/10.1021/jf801957h.

D'Agostino, L., Di Pietro, M., Di Luccia, A., 2005. Nuclear aggregates of polyamines are supramolecular structures that play a crucial role in genomic DNA protection and conformation. FEBS J. 272, 3777–3787. https://doi.org/10.1111/j.1742-4658.2005.04782.x.

Dai, J., Punchihewa, C., Ambrus, A., Chen, D., Jones, R.A., Yang, D., 2007. Structure of the intramolecular human telomeric G-quadruplex in potassium solution: a novel adenine triple formation. Nucleic Acids Res. 35, 2440–2450. https://doi.org/10.1093/nar/gkm009.

Dai, R., Wang, X., Wang, Z., Mu, S., Liao, J., Wen, Y., Lv, J., Huang, K., Xiong, X., 2019. A sensitive and label-free sensor for melamine and iodide by target-regulating the formation of G-quadruplex. Microchem. J. 146, 592–599. https://doi.org/10.1016/j.microc.2019.01.044.

Dasgupta, S., Shelke, S.A., Li, N.S., Piccirilli, J.A., 2015. Spinach RNA aptamer detects lead(ii) with high selectivity. Chem. Commun. 51, 9034–9037. https://doi.org/10.1039/c5cc01526j.

David, W.M., Brodbelt, J., Kerwin, S.M., Wang Thomas, P., 2002. Investigation of quadruplex oligonucleotide - drug interactions by electrospray ionization mass spectrometry. Anal. Chem. 74, 2029–2033. https://doi.org/10.1021/ac011283w.

Day, H.A., Pavlou, P., Waller, Z.A.E., 2014. I-Motif DNA: structure, stability and targeting with ligands. Bioorg. Med. Chem. 22, 4407–4418. https://doi.org/10.1016/j.bmc.2014.05.047.

del Villar-Guerra, R., Trent, J.O., Chaires, J.B., 2018. G-quadruplex secondary structure obtained from circular dichroism spectroscopy. Angew. Chem. Int. Ed. 57, 7171–7175. https://doi.org/10.1002/anie.201709184.

Deng, B., Lin, Y., Wang, C., Li, F., Wang, Z., Zhang, H., Li, X.F., Le, X.C., 2014. Aptamer binding assays for proteins: the thrombin example-A review. Anal. Chim. Acta 837, 1–15. https://doi.org/10.1016/j.aca.2014.04.055.

Feng, L., Chen, Y., Ren, J., Qu, X., 2011. A graphene functionalized electrochemical aptasensor for selective label-free detection of cancer cells. Biomaterials 32, 2930–2937. https://doi.org/10.1016/j.biomaterials.2011.01.002.

Franceschin, M., Lombardo, C.M., Pascucci, E., D'Ambrosio, D., Micheli, E., Bianco, A., Ortaggi, G., Savino, M., 2008. The number and distances of positive charges of polyamine side chains in a series of perylene diimides significantly influence their ability to induce G-quadruplex structures and inhibit human telomerase. Bioorg. Med. Chem. 16, 2292–2304. https://doi.org/10.1016/j.bmc.2007.11.065.

Frank-Kamenetskii, M.D., Mirkin, S.M., 1995. Triplex DNA structures. Annu. Rev. Biochem. 64, 65–95. https://doi.org/10.1146/annurev.bi.64.070195.000433.

Frank-Kamenetskii, M.D., Mirkin, S.M., Neidle, S., Parkinson, G.N., 2003. The structure of telomeric DNA. Curr. Opin. Struct. Biol. 13, 275–283. https://doi.org/10.1016/S0959-440X(03)00072-1.

Fu, Y., Wang, X., Zhang, J., Xiao, Y., Li, W., Wang, J., 2011. Orderly Microaggregates of G-/C-rich oligonucleotides associated with spermine. Biomacromolecules 12, 747–756. https://doi.org/10.1021/bm101372h.

Fujii, T., Podbevšek, P., Plavec, J., Sugimoto, N., 2017. Effects of metal ions and cosolutes on G-quadruplex topology. J. Inorg. Biochem. 166, 190–198. https://doi.org/10.1016/j.jinorgbio.2016.09.001.

Fulton, A.B., 1982. How crowded is the cytoplasm? Cell 30, 345–347. https://doi.org/10.1016/0092-8674(82)90231-8.

Galer, P., Wang, B., Šket, P., Plavec, J., 2016. Reversible pH switch of two-quartet G-quadruplexes formed by human telomere. Angew. Chem. Int. Ed. 55 https://doi.org/10.1002/anie.201507569, 1993–1997.

Gao, S., Hu, W., Zheng, X., Cai, S., Wu, J., 2019. Functionalized aptamer with an antiparallel G-quadruplex: structural remodeling, recognition mechanism, and diagnostic applications targeting CTGF. Biosens. Bioelectron. 142, 111475. https://doi.org/10.1016/j.bios.2019.111475.

Guet, D., Burns, L.T., Maji, S., Boulanger, J., Hersen, P., Wente, S.R., Salamero, J., Dargemont, C., 2015. Combining Spinach-tagged RNA and gene localization to image gene expression in live yeast. Nat. Commun. 6 https://doi.org/10.1038/ncomms9882.

Ha, H.C., Sirisoma, N.S., Kuppusamy, P., Zweier, J.L., Woster, P.M., Casero, R.A., 1998. The natural polyamine spermine functions directly as a free radical scavenger. Proc. Natl. Acad. Sci. U.S.A. 95, 11140–11145. https://doi.org/10.1073/pnas.95.19.11140.

Hu, Y., Cecconello, A., Idili, A., Ricci, F., Willner, I., 2017. Triplex DNA nanostructures: from basic properties to applications. Angew. Chem. Int. Ed. 56, 15210–15233. https://doi.org/10.1002/anie.201701868.

Huang, H., Suslov, N.B., Li, N.S., Shelke, S.A., Evans, M.E., Koldobskaya, Y., Rice, P.A., Piccirilli, J.A., 2014. A G-quadruplex-containing RNA activates fluorescence in a GFP-like fluorophore. Nat. Chem. Biol. 10, 686–691. https://doi.org/10.1038/nchembio.1561.

Huizenga, D.E., Szostak, J.W., 1995. A DNA aptamer that binds adenosine and ATP. Biochemistry 34, 656–665. https://doi.org/10.1021/bi00002a033.

Ikebukuro, K., Kiyohara, C., Sode, K., 2004. Electrochemical detection of protein using a double aptamer sandwich. Anal. Lett. 37, 2901–2909. https://doi.org/10.1081/AL-200035778.

Ji, D., Wang, H., Ge, J., Zhang, L., Li, J., Bai, D., Chen, J., Li, Z., 2017. Label-free and rapid detection of ATP based on structure switching of aptamers. Anal. Biochem. 526, 22–28. https://doi.org/10.1016/j.ab.2017.03.011.

Ji, R., Niu, W., Chen, S., Xu, W., Ji, X., Yuan, L., Zhao, H., Geng, M., Qiu, J., Li, C., 2019. Target-inspired Pb2+-dependent DNAzyme for ultrasensitive electrochemical sensor based on MoS2-AuPt nanocomposites and hemin/G-quadruplex DNAzyme as signal amplifier. Biosens. Bioelectron. 144, 111560. https://doi.org/10.1016/j.bios.2019.111560.

Jing, N., Rando, R.F., Pommier, Y., Hogan, M.E., 1997. Ion selective Folding of loop domains in a potent anti-HIV oligonucleotide. Biochemistry 36, 12498–12505. https://doi.org/10.1021/bi962798y.

Kan, Z.Y., Yao, Y., Wang, P., Li, X.H., Hao, Y.H., Tan, Z., 2006. Molecular crowding induces telomere G-quadruplex formation under salt-deficient conditions and enhances its competition with duplex formation. Angew. Chem. Int. Ed. 45, 1629–1632. https://doi.org/10.1002/anie.200502960.

Keniry, M.A., 2003. A comparison of the association of spermine with duplex and quadruplex DNA by NMR. FEBS Lett. 542, 153–158. https://doi.org/10.1016/S0014-5793(03)00373-9.

Keniry, M.A., Owen, E.A., 2013. Insight into the molecular recognition of spermine by DNA quadruplexes from an NMR study of the association of spermine with the thrombin-binding aptamer. J. Mol. Recogn. 26, 308–317. https://doi.org/10.1002/jmr.2274.

Kosman, J., Juskowiak, B., 2011. Peroxidase-mimicking DNAzymes for biosensing applications: a review. Anal. Chim. Acta 707, 7–17. https://doi.org/10.1016/j.aca.2011.08.050.

Lane, A.N., Chaires, J.B., Gray, R.D., Trent, J.O., 2008. Stability and kinetics of G-quadruplex structures. Nucleic Acids Res. 36, 5482–5515. https://doi.org/10.1093/nar/gkn517.

Lee, J.A., Derosa, M.C., 2010. A pH-driven DNA switch based on the A+·G mispair. Chem. Commun. 46, 418–420. https://doi.org/10.1039/b918725a.

Li, C., Chen, H., Chen, Q., Shi, H., Yang, X., Wang, K., Liu, J., 2020. Lipophilic G-quadruplex isomers as biomimetic ion channels for conformation-dependent selective transmembrane transport. Anal. Chem. 92, 10169–10176. https://doi.org/10.1021/acs.analchem.0c02222.

Li, C., Chen, H., Zhou, L., Shi, H., He, X., Yang, X., Wang, K., Liu, J., 2019. Single-stranded DNA designed lipophilic G-quadruplexes as transmembrane channels for switchable potassium transport. Chem. Commun. 55, 12004–12007. https://doi.org/10.1039/c9cc04176a.

Li, C.L., Huang, C.C., Chen, W.H., Chiang, C.K., Chang, H.T., 2012. Peroxidase mimicking DNA-gold nanoparticles for fluorescence detection of the lead ions in blood. Analyst 137, 5222–5228. https://doi.org/10.1039/c2an35599j.

Li, C.L., Liu, K.T., Lin, Y.W., Chang, H.T., 2011. Fluorescence detection of lead(II) ions through their induced catalytic activity of DNAzymes. Anal. Chem. 83, 225–230. https://doi.org/10.1021/ac1028787.

Li, H., 2019. Mass spectroscopic study of G-quadruplex. Methods Mol. Biol. 2035, 105–116. https://doi.org/10.1007/978-1-4939-9666-7_6.

Li, J., Correia, J.J., Wang, L., Trent, J.O., Chaires, J.B., 2005. Not so crystal clear: the structure of the human telomere G-quadruplex in solution differs from that present in a crystal. Nucleic Acids Res. 33, 4649–4659. https://doi.org/10.1093/nar/gki782.

Li, T., Wang, E., Dong, S., 2010. Lead(II)-induced allosteric G-quadruplex DNAzyme as a Colorimetric and chemiluminescence sensor for highly sensitive and selective Pb2+ detection. Anal. Chem. 82, 1515–1520. https://doi.org/10.1021/ac902638v.

Liang, G., Man, Y., Li, A., Jin, X., Liu, X., Pan, L., 2017. DNAzyme-based biosensor for detection of lead ion: a review. Microchem. J. 131, 145–153. https://doi.org/10.1016/j.microc.2016.12.010.

Liu, H., Ma, C., Ning, F., Chen, H., He, H., Wang, K., Wang, J., 2017. A facile label-free G-quadruplex based fluorescent aptasensor method for rapid detection of ATP. Spectrochim. Acta Part A Mol. Biomol. Spectrosc. 175, 164–167. https://doi.org/10.1016/j.saa.2016.12.033.

Liu, W., Zhu, H., Zheng, B., Cheng, S., Fu, Y., Li, W., Lau, T.C., Liang, H., 2012. Kinetics and mechanism of G-quadruplex formation and conformational switch in a G-quadruplex of PS2.M induced by Pb2+. Nucleic Acids Res. 40, 4229–4236. https://doi.org/10.1093/nar/gkr1310.

Lubitz, I., Zikich, D., Kotlyar, A., 2010. Specific high-affinity binding of thiazole orange to triplex and G-quadruplex DNA. Biochemistry 49, 3567–3574. https://doi.org/10.1021/bi1000849.

Luu, K.N., Phan, A.T., Kuryavyi, V., Lacroix, L., Patel, D.J., 2006. Structure of the human telomere in K+ solution: an intramolecular (3 + 1) G-quadruplex scaffold. J. Am. Chem. Soc. 128, 9963–9970. https://doi.org/10.1021/ja062791w.

Lv, M., Guo, Y., Ren, J., Wang, E., 2019. Exploration of intramolecular split G-quadruplex and its analytical applications. Nucleic Acids Res. 47, 9502–9510. https://doi.org/10.1093/nar/gkz749.

Ma, D.L., Wang, W., Mao, Z., Kang, T.S., Han, Q. Bin, Chan, P.W.H., Leung, C.H., 2017. Utilization of G-quadruplex-forming aptamers for the construction of luminescence sensing platforms. Chempluschem 82, 8–17. https://doi.org/10.1002/cplu.201600036.

Ma, G., Yu, Z., Zhou, W., Li, Y., Fan, L., Li, X., 2019. Investigation of Na+ and K+ competitively binding with a G-quadruplex and discovery of a stable K+-Na+-Quadruplex. J. Phys. Chem. B 123, 5405–5411. https://doi.org/10.1021/acs.jpcb.9b02823.

Ma, Y., Iida, K., Nagasawa, K., 2020. Topologies of G-quadruplex: biological functions and regulation by ligands. Biochem. Biophys. Res. Commun. 531, 3–17. https://doi.org/10.1016/j.bbrc.2019.12.103.

Macaya, R.F., Schultze, P., Smith, F.W., Roe, J.A., Feigon, J., 1993. Thrombin-binding DNA aptamer forms a unimolecular quadruplex structure in solution. Proc. Natl. Acad. Sci. U.S.A. 90, 3745–3749. https://doi.org/10.1073/pnas.90.8.3745.

Maizels, N., Gray, L.T., 2013. The G4 genome. PLoS Genet. 9 https://doi.org/10.1371/journal.pgen.1003468.

Matsugami, A., Xu, Y., Noguchi, Y., Sugiyama, H., Katahira, M., 2007. Structure of a human telomeric DNA sequence stabilized by 8-bromoguanosine substitutions, as determined by NMR in a K+ solution. FEBS J. 274, 3545–3556. https://doi.org/10.1111/j.1742-4658.2007.05881.x.

McConnell, E.M., Bolzon, R., Mezin, P., Frahm, G., Johnston, M., DeRosa, M.C., 2016. PHAST (pH-Driven aptamer switch for thrombin) catch-and-release of target protein. Bioconjugate Chem. 27, 1493–1499. https://doi.org/10.1021/acs.bioconjchem.6b00124.

McLuckie, K.I.E., Di Antonio, M., Zecchini, H., Xian, J., Caldas, C., Krippendorff, B.F., Tannahill, D., Lowe, C., Balasubramanian, S., 2013. G-quadruplex DNA as a molecular target for induced synthetic lethality in cancer cells. J. Am. Chem. Soc. 135, 9640–9643. https://doi.org/10.1021/ja404868t.

Miyoshi, D., Karimata, H., Sugimoto, N., 2006. Hydration regulates thermodynamics of G-quadruplex formation under molecular crowding conditions. J. Am. Chem. Soc. 128, 7957–7963. https://doi.org/10.1021/ja061267m.

Miyoshi, D., Karimata, H., Sugimoto, N., 2005. Drastic effect of a single base difference between human and Tetrahymena telomere sequences on their structures under molecular crowding conditions. Angew. Chem. Int. Ed. 44, 3740–3744. https://doi.org/10.1002/anie.200462667.

Miyoshi, D., Nakao, A., Sugimoto, N., 2002. Molecular crowding regulates the structural switch of the DNA G-quadruplex. Biochemistry 41, 15017–15024. https://doi.org/10.1021/bi020412f.

Miyoshi, D., Sugimoto, N., 2008. Molecular crowding effects on structure and stability of DNA. Biochimie 90, 1040–1051. https://doi.org/10.1016/j.biochi.2008.02.009.

Mohanty, J., Barooah, N., Dhamodharan, V., Harikrishna, S., Pradeepkumar, P.I., Bhasikuttan, A.C., 2013. Thioflavin T as an efficient inducer and selective fluorescent sensor for the human telomeric G-quadruplex DNA. J. Am. Chem. Soc. 135, 367–376. https://doi.org/10.1021/ja309588h.

Moye, A.L., Porter, K.C., Cohen, S.B., Phan, T., Zyner, K.G., Sasaki, N., Lovrecz, G.O., Beck, J.L., Bryan, T.M., 2015. Telomeric G-quadruplexes are a substrate and site of localization for human telomerase. Nat. Commun. 6 https://doi.org/10.1038/ncomms8643.

Nakano, S., Miyoshi, D., Sugimoto, N., 2014. Effects of molecular crowding on the structures, interactions, and functions of. Nucleic Acids. Chem. Rev. 114, 2733–2758. https://doi.org/10.1021/cr400113m.

Nakayama, S., Luo, Y., Zhou, J., Dayie, T.K., Sintim, H.O., 2012. Nanomolar fluorescent detection of c-di-GMP using a modular aptamer strategy. Chem. Commun. 48, 9059–9061. https://doi.org/10.1039/c2cc34379g.

Nicoludis, J.M., Barrett, S.P., Mergny, J.L., Yatsunyk, L.A., 2012. Interaction of human telomeric DNA with N-methyl mesoporphyrin IX. Nucleic Acids Res. 40, 5432–5447. https://doi.org/10.1093/nar/gks152.

Nishio, M., Matsumoto, D., Kato, Y., Abe, K., Lee, J., Tsukakoshi, K., Yamagishi, A., Nakamura, C., Ikebukuro, K., 2017. DNA aptamers against FokI nuclease domain for genome editing applications. Biosens. Bioelectron. 93, 26–31. https://doi.org/10.1016/j.bios.2016.11.042.

Nonaka, Y., Sode, K., Ikebukuro, K., 2010. Screening and improvement of an anti-VEGF DNA aptamer. Molecules 15, 215–225. https://doi.org/10.3390/molecules15010215. www.mdpi.com/journal/molecules.

Ogihara, K., Savory, N., Abe, K., Yoshida, W., Asahi, M., Kamohara, S., Ikebukuro, K., 2015. DNA aptamers against the Cry j 2 allergen of Japanese cedar pollen for biosensing applications. Biosens. Bioelectron. 63, 159–165. https://doi.org/10.1016/j.bios.2014.07.030.

Ohnmacht, S.A., Marchetti, C., Gunaratnam, M., Besser, R.J., Haider, S.M., Di Vita, G., Lowe, H.L., Mellinas-Gomez, M., Diocou, S., Robson, M., Šponer, J., Islam, B., Barbara Pedley, R., Hartley, J.A., Neidle, S., 2015. A G-quadruplex-binding compound showing anti-tumour activity in an in vivo model for pancreatic cancer. Sci. Rep. 5, 1–11. https://doi.org/10.1038/srep11385.

Ong, W.Q., Citron, Y.R., Sekine, S., Huang, B., 2017. Live Cell imaging of endogenous mRNA Using RNA-Based fluorescence "turn-on" probe. ACS Chem. Biol. 12, 200–205. https://doi.org/10.1021/acschembio.6b00586.

Ou, T.M., Lu, Y.J., Tan, J.H., Huang, Z.S., Wong, K.Y., Gu, L.Q., 2008. G-quadruplexes: targets in anticancer drug design. ChemMedChem 3, 690–713. https://doi.org/10.1002/cmdc.200700300.

Paige, J.S., Nguyen-Duc, T., Song, W., Jaffrey, S.R., 2012. Fluorescence imaging of cellular metabolites with RNA. Science (80-.) 335, 1194. https://doi.org/10.1126/science.1218298.

Paige, J.S., Wu, K.Y., Jaffrey, S.R., 2011. RNA mimics of green fluorescent protein. Science 333, 642–646. https://doi.org/10.1126/science.1207339.

Paramasivan, S., Rujan, I., Bolton, P.H., 2007. Circular dichroism of quadruplex DNAs: applications to structure, cation effects and ligand binding. Methods 43, 324–331. https://doi.org/10.1016/j.ymeth.2007.02.009.

Parkinson, G.N., Lee, M.P.H., Neidle, S., 2002. Crystal structure of parallel quadruplexes from human telomeric DNA. Nature 417, 876–880. https://doi.org/10.1038/nature755.

Petraccone, L., Pagano, B., Giancola, C., 2012. Studying the effect of crowding and dehydration on DNA G-quadruplexes. Methods 57, 76–83. https://doi.org/10.1016/j.ymeth.2012.02.011.

Pfohl-Leszkowicz, A., Manderville, R.A., 2007. Ochratoxin A: an overview on toxicity and carcinogenicity in animals and humans. Mol. Nutr. Food Res. 51, 61–99. https://doi.org/10.1002/mnfr.200600137.

Phan, A.T., 2010. Human telomeric G-quadruplex: structures of DNA and RNA sequences. FEBS J. 277, 1107–1117. https://doi.org/10.1111/j.1742-4658.2009.07464.x.

Phan, A.T., Kuryavyi, V., Luu, K.N., Patel, D.J., 2007. Structure of two intramolecular G-quadruplexes formed by natural human telomere sequences in K+ solution. Nucleic Acids Res. 35, 6517–6525. https://doi.org/10.1093/nar/gkm706.

Phan, A.T., Modi, Y.S., Patel, D.J., 2004. Propeller-type parallel-stranded G-quadruplexes in the human c-myc promoter. J. Am. Chem. Soc. 126, 8710–8716. https://doi.org/10.1021/ja048805k.

Platella, C., Riccardi, C., Montesarchio, D., Roviello, G.N., Musumeci, D., 2017. G-quadruplex-based aptamers against protein targets in therapy and diagnostics. Biochim. Biophys. Acta Gen. Subj. 1861, 1429–1447. https://doi.org/10.1016/j.bbagen.2016.11.027.

Qi, C., Bing, T., Mei, H., Yang, X., Liu, X., Shangguan, D., 2013. G-quadruplex DNA aptamers for zeatin recognizing. Biosens. Bioelectron. 41, 157–162. https://doi.org/10.1016/j.bios.2012.08.004.

Qi, C., Zhang, N., Yan, J., Liu, X., Bing, T., 2014. RSC Advances Activity enhancement of G-quadruplex/hemin DNAzyme by spermine †, 1441–1448. https://doi.org/10.1039/c3ra45429k.

Rodriguez, R., Miller, K.M., Forment, J.V., Bradshaw, C.R., Nikan, M., Britton, S., Oelschlaegel, T., Xhemalce, B., Balasubramanian, S., Jackson, S.P., 2012. Small-molecule-induced DNA damage identifies alternative DNA structures in human genes. Nat. Chem. Biol. 8, 301–310. https://doi.org/10.1038/nchembio.780.

Roxo, C., Kotkowiak, W., Pasternak, A., 2019. G-quadruplex-forming aptamers—characteristics, applications, and perspectives. Molecules 24. https://doi.org/10.3390/molecules24203781.

Salvati, E., Scarsella, M., Porru, M., Rizzo, A., Iachettini, S., Tentori, L., Graziani, G., D'Incalci, M., Stevens, M.F.G., Orlandi, A., Passeri, D., Gilson, E., Zupi, G., Leonetti, C., Biroccio, A., 2010. PARP1 is activated at telomeres upon G4 stabilization: possible target for telomere-based therapy. Oncogene 29, 6280–6293. https://doi.org/10.1038/onc.2010.344.

Sen, D., Gilbert, W., 1988. Formation of parallel four-stranded complexes by guanine-rich motifs in DNA and its implications for meiosis. Nature 334, 364–366. https://doi.org/10.1038/334364a0.

Shen, G., Zhang, H., Yang, C., Yang, Q., Tang, Y., 2017. Thrombin ultrasensitive detection based on chiral supramolecular assembly signal-amplified strategy induced by thrombin-binding aptamer. Anal. Chem. 89, 548–551. https://doi.org/10.1021/acs.analchem.6b04247.

Smirnov, I.P., Kolganova, N.A., Surzhikov, S.A., Grechishnikova, I.V., Novikov, R.A., Timofeev, E.N., 2020. Folding topology, structural polymorphism, and dimerization of intramolecular DNA G-quadruplexes with inverted polarity strands and non-natural loops. Int. J. Biol. Macromol. 162, 1972–1981. https://doi.org/10.1016/j.ijbiomac.2020.08.097.

Song, W., Strack, R.L., Jaffrey, S.R., 2013. Imaging bacterial protein expression using genetically encoded RNA sensors. Nat. Methods 10, 873–875. https://doi.org/10.1038/nmeth.2568.

Spiegel, J., Adhikari, S., Balasubramanian, S., 2020. The structure and function of DNA G-quadruplexes. Trends Chem. 2, 123–136. https://doi.org/10.1016/j.trechm.2019.07.002.

Takahashi, S., Yamamoto, J., Kitamura, A., Kinjo, M., Sugimoto, N., 2019. Characterization of intracellular crowding environments with topology-based DNA quadruplex sensors. Anal. Chem. 2586–2590. https://doi.org/10.1021/acs.analchem.8b04177.

Tang, X., Wang, Y., Zhou, L., Zhang, W., Yang, S., Yu, L., Zhao, S., Chang, K., Chen, M., 2020. Strand displacement-triggered G-quadruplex/rolling circle amplification strategy for the ultra-sensitive electrochemical sensing of exosomal microRNAs. Microchim. Acta 187. https://doi.org/10.1007/s00604-020-4143-9.

Tateishi-Karimata, H., Banerjee, D., Ohyama, T., Matsumoto, S., Miyoshi, D., Nakano, S. ich, Sugimoto, N., 2020. Hydroxyl groups in cosolutes regulate the G-quadruplex topology of telomeric DNA. Biochem. Biophys. Res. Commun. 525, 177–183. https://doi.org/10.1016/j.bbrc.2020.02.045.

Thomas, T., Thomas, T.J., 2001. Polyamines in cell growth and cell death: molecular mechanisms and therapeutic applications. Cell. Mol. Life Sci. 58, 244–258. https://doi.org/10.1007/PL00000852.

Tong, X., Lan, W., Zhang, X., Wu, H., Liu, M., Cao, C., 2011. Solution structure of all parallel G-quadruplex formed by the oncogene RET promoter sequence. Nucleic Acids Res. 39, 6753–6763. https://doi.org/10.1093/nar/gkr233.

Travascio, P., Li, Y., Sen, D., 1998. DNA-enhanced peroxidase activity of a DNA aptamer-hemin complex. Chem. Biol. 5, 505–517. https://doi.org/10.1016/S1074-5521(98)90006-0.

Tsukakoshi, K., Ikuta, Y., Abe, K., Yoshida, W., Iida, K., Ma, Y., Nagasawa, K., Sode, K., Ikebukuro, K., 2016. Structural regulation by a G-quadruplex ligand increases binding abilities of G-quadruplex-forming aptamers. Chem. Commun. 52, 12646–12649. https://doi.org/10.1039/c6cc07552e.

Umar, M.I., Ji, D., Chan, C.Y., Kwok, C.K., 2019. G-quadruplex-based fluorescent turn-on ligands and aptamers: from development to applications, Molecules. https://doi.org/10.3390/molecules24132416.

Wang, Y., Fang, Z., Ning, G., Mao, S., Wu, Y., Wu, S., Liu, G.-Q., 2019. G-quadruplex-bridged triple-helix aptamer probe strategy: a label-free chemiluminescence biosensor for ochratoxin A. Sensor. Actuator. B Chem. 298, 126867. https://doi.org/10.1016/j.snb.2019.126867.

Wang, Y., Patel, D.J., 1993. Solution structure of the human telomeric repeat d[AG3 (T2AG3)3] G-tetraplex. Structure 1, 263–282. https://doi.org/10.1016/0969-2126(93)90015-9.

Wang, Y., Patel, D.J., 1992. Guanine residues in d(T2AG3) and d(T2G4) form parallel-stranded potassium cation stabilized G-quadruplexes with anti glycosidic torsion angles in solution. Biochemistry 31, 8112–8119. https://doi.org/10.1021/bi00150a002.

Wang, Z., Zhao, J., Bao, J., Dai, Z., 2016. Construction of metal-ion-free G-quadruplex-hemin DNAzyme and its application in S1 nuclease detection. ACS Appl. Mater. Interfaces 8, 827–833. https://doi.org/10.1021/acsami.5b10165.

Xi, H., Juhas, M., Zhang, Y., 2020. G-quadruplex based biosensor: a potential tool for SARS-CoV-2 detection. Biosens. Bioelectron. 167, 112494. https://doi.org/10.1016/j.bios.2020.112494.

Xu, L., Chen, Y., Zhang, R., Gao, T., Zhang, Y., Shen, X., Pei, R., 2017. A highly sensitive turn-on fluorescent sensor for Ba2+ based on G-quadruplexes. J. Fluoresc. 27, 569–574. https://doi.org/10.1007/s10895-016-1984-z.

Xu, S., Li, Q., Xiang, J., Yang, Q., Sun, H., Guan, A., Wang, L., Liu, Y., Yu, L., Shi, Y., Chen, H., Tang, Y., 2015. Directly lighting up RNA G-quadruplexes from test tubes to living human cells. Nucleic Acids Res. 43, 9575–9586. https://doi.org/10.1093/nar/gkv1040.

Yan, Y.Y., Tan, J.H., Lu, Y.J., Yan, S.C., Wong, K.Y., Li, D., Gu, L.Q., Huang, Z.S., 2013. G-Quadruplex conformational change driven by pH variation with potential application as a nanoswitch. Biochim. Biophys. Acta Gen. Subj. 1830, 4935–4942. https://doi.org/10.1016/j.bbagen.2013.06.019.

Yang, H., Zhou, Y., Liu, J., 2020. G-quadruplex DNA for construction of biosensors. TrAC Trends Anal. Chem. (Reference Ed.) 132, 116060. https://doi.org/10.1016/j.trac.2020.116060.

Yang, Y., Zhu, W., Feng, L., Chao, Y., Yi, X., Dong, Z., Yang, K., 2018. G - quadruplex-based nanoscale coordination polymers to modulate tumor hypoxia and achieve nuclear-targeted drug delivery for enhanced photodynamic therapy, 2–10. https://doi.org/10.1021/acs.nanolett.8b02732.

Ye, T., Gao, H., Zhang, Q., Yan, C., Yu, Y., Fei, Y., Gao, L., Zhou, X., Shao, Y., 2019a. Polarity inversion sensitized G-quadruplex metal sensors with K+ tolerance. Biosens. Bioelectron. 145, 111703. https://doi.org/10.1016/j.bios.2019.111703.

Ye, T., Gao, H., Zhang, Q., Yan, C., Yu, Y., Fei, Y., Gao, L., Zhou, X., Shao, Y., 2019b. Polarity inversion sensitized G-quadruplex metal sensors with K+ tolerance. Biosens. Bioelectron. 145, 111703. https://doi.org/10.1016/j.bios.2019.111703.

Ying, Z.M., Tu, B., Liu, L., Tang, H., Tang, L.J., Jiang, J.H., 2018. Spinach-based fluorescent light-up biosensors for multiplexed and label-free detection of microRNAs. Chem. Commun. 54, 3010–3013. https://doi.org/10.1039/c8cc00123e.

Ying, Z.M., Wu, Z., Tu, B., Tan, W., Jiang, J.H., 2017. Genetically encoded fluorescent RNA sensor for ratiometric imaging of MicroRNA in living tumor cells. J. Am. Chem. Soc. 139, 9779–9782. https://doi.org/10.1021/jacs.7b04527.

Yoshida, W., Mochizuki, E., Takase, M., Hasegawa, H., Morita, Y., Yamazaki, H., Sode, K., Ikebukuro, K., 2009. Selection of DNA aptamers against insulin and construction of an aptameric enzyme subunit for insulin sensing. Biosens. Bioelectron. 24, 1116–1120. https://doi.org/10.1016/j.bios.2008.06.016.

Yu, Z., Zhou, W., Han, J., Li, Y., Fan, L., Li, X., 2016. Na+-Induced conformational change of Pb2+-stabilized G-quadruplex and its influence on Pb2+ detection. Anal. Chem. 88, 9375–9380. https://doi.org/10.1021/acs.analchem.6b02466.

Yu, Z., Zhou, W., Ma, G., Li, Y., Fan, L., Li, X., Lu, Y., 2018. Insights into the competition between K+ and Pb2+ binding to a G-quadruplex and discovery of a novel K+-Pb2+-quadruplex intermediate. J. Phys. Chem. B 122, 9382–9388. https://doi.org/10.1021/acs.jpcb.8b08161.

Zahler, A.M., Williamson, J.R., Cech, T.R., Prescott, D.M., 1991. Inhibition of telomerase by G-quartet DMA structures. Nature 350, 718–720. https://doi.org/10.1038/350718a0.

Zhang, J., Fei, J., Leslie, B.J., Han, K.Y., Kuhlman, T.E., Ha, T., 2015. Tandem spinach array for mRNA imaging in living bacterial cells. Sci. Rep. 5, 1–9. https://doi.org/10.1038/srep17295.

Zhang, L., Zhang, X., Feng, P., Han, Q., Liu, W., Lu, Y., Song, C., Li, F., 2020. Photodriven regeneration of G-quadruplex aptasensor for sensitively detecting thrombin. Anal. Chem. 92, 7419–7424. https://doi.org/10.1021/acs.analchem.0c00380.

Zhang, M.L., Xu, Y.P., Kumar, A., Zhang, Y., Wu, W.Q., 2019. Studying the potassium-induced G-quadruplex DNA folding process using microscale thermophoresis. Biochemistry 58, 3955–3959. https://doi.org/10.1021/acs.biochem.9b00447.

Zhang, S., Sun, H., Wang, L., Liu, Y., Chen, H., Li, Q., Guan, A., Liu, M., Tang, Y., 2018. Real-time monitoring of DNA G-quadruplexes in living cells with a small-molecule fluorescent probe. Nucleic Acids Res. 46, 7522–7532. https://doi.org/10.1093/nar/gky665.

Zhang, S., Zhang, R., Ma, B., Qiu, J., Li, J., Sang, Y., Liu, W., Liu, H., 2016. Specific detection of potassium ion in serum by a modified G-quadruplex method. RSC Adv. 6, 41999–42007. https://doi.org/10.1039/c6ra04046b.

Zhou, J., Tateishi-Karimata, H., Mergny, J.L., Cheng, M., Feng, Z., Miyoshi, D., Sugimoto, N., Li, C., 2016. Reevaluation of the stability of G-quadruplex structures under crowding conditions. Biochimie 121, 204–208. https://doi.org/10.1016/j.biochi.2015.12.012.

Zhou, W., Saran, R., Liu, J., 2017. Metal sensing by DNA. Chem. Rev. 117, 8272–8325. https://doi.org/10.1021/acs.chemrev.7b00063.

Zimmer, J., Tacconi, E.M.C., Folio, C., Badie, S., Porru, M., Klare, K., Tumiati, M., Markkanen, E., Halder, S., Ryan, A., Jackson, S.P., Ramadan, K., Kuznetsov, S.G., Biroccio, A., Sale, J.E., Tarsounas, M., 2016. Targeting BRCA1 and BRCA2 deficiencies with G-quadruplex-interacting compounds. Mol. Cell 61, 449–460. https://doi.org/10.1016/j.molcel.2015.12.004.